RESEARCH ARTICLE

The brain of *Cataglyphis* ants: Neuronal organization and visual projections

Jens Habenstein[1] | Emad Amini[2] | Kornelia Grübel[1] | Basil el Jundi[1] |
Wolfgang Rössler[1]

[1]Biocenter, Behavioral Physiology and Sociobiology (Zoology II), University of Würzburg, Würzburg, Germany

[2]Biocenter, Neurobiology and Genetics, University of Würzburg, Würzburg, Germany

Correspondence
Basil el Jundi and Wolfgang Rössler, Biocenter, Behavioral Physiology and Sociobiology (Zoology II), University of Würzburg, Am Hubland, Würzburg 97074, Germany.
Email: basil.el-jundi@uni-wuerzburg.de (B. J.) and roessler@biozentrum.uni-wuerzburg.de (W. R.)

Abstract

Cataglyphis ants are known for their outstanding navigational abilities. They return to their inconspicuous nest after far-reaching foraging trips using path integration, and whenever available, learn and memorize visual features of panoramic sceneries. To achieve this, the ants combine directional visual information from celestial cues and panoramic scenes with distance information from an intrinsic odometer. The largely vision-based navigation in *Cataglyphis* requires sophisticated neuronal networks to process the broad repertoire of visual stimuli. Although *Cataglyphis* ants have been subjected to many neuroethological studies, little is known about the general neuronal organization of their central brain and the visual pathways beyond major circuits. Here, we provide a comprehensive, three-dimensional neuronal map of synapse-rich neuropils in the brain of *Cataglyphis nodus* including major connecting fiber systems. In addition, we examined neuronal tracts underlying the processing of visual information in more detail. This study revealed a total of 33 brain neuropils and 30 neuronal fiber tracts including six distinct tracts between the optic lobes and the cerebrum. We also discuss the importance of comparative studies on insect brain architecture for a profound understanding of neuronal networks and their function.

----

1 | INTRODUCTION

Ants of the genus *Cataglyphis* (Foerster 1850) are thermophilic and live in arid zones of Central and North Africa, the Mediterranean, Middle East, and in Central Asia. Their natural habitats comprise deserts, steppes, and Mediterranean landscapes (Agosti, 1990). Due to high surface temperatures and scarce food sources, *Cataglyphis* ants are solitary foragers and do not employ pheromone trails to recruit nestmates (Ruano, Tinaut, & Soler, 2000). The ants predominantly rely on visual cues during far-reaching foraging trips that may span over remarkable distances (reviewed by: Wehner, 2003; Buehlmann, Graham, Hansson, & Knaden, 2014; Huber & Knaden, 2015). Even in environments that lack distinct panoramic features, *Cataglyphis* foragers find their way back to their nest along an almost straight line using path integration (for reviews, see Ronacher, 2008; Wehner, 2009). For path integration, the distance and directional information have to be continuously updated (and stored) during outbound trips. In *Cataglyphis*, the distance information is encoded by a stride-integration mechanism in combination with optic-flow perception (Pfeffer & Wittlinger, 2016; Wittlinger, Wehner, & Wolf, 2006; Wolf, Wittlinger, & Pfeffer, 2018), and the directional information by celestial cues such as the polarization pattern, the position of the sun, and the spectral gradient (Lebhardt & Ronacher, 2014, 2015; Wehner, 1997; Wehner & Muller, 2006). Even though path integration works without any landmark information, *Cataglyphis* ants use the panoramic skyline and visual landmarks of their surroundings, whenever available, to minimize errors (Collett, Dillmann, Giger, & Wehner, 1992; Wehner, Hoinville, Cruse, & Cheng, 2016; Wehner, Michel, & Antonsen, 1996; Wehner & Räber, 1979). The combination of path integration and landmark guidance generates a robust navigational compass (Knaden & Wehner, 2005) and provides a most successful form of navigation. More recently, *Cataglyphis nodus* (Brullé 1833), the species in the focus of our present study, was shown to use a magnetic compass for calibrating their visual compasses during naïve learning (exploration) walks that the ants perform upon leaving the nest for the first time and before heading out on first foraging trips (Fleischmann, Grob, Müller, Wehner, & Rössler, 2018; reviewed by: Grob, Fleischmann, & Rössler, 2019).

Both path integration and landmark guidance require sophisticated processing and storage of different visual information in the relatively small brain of the ants. Recent studies have mainly focused on two visual pathways—one projects to the central complex (CX), the other to the mushroom bodies (MBs) (for reviews, see Grob et al., 2019; Rössler, 2019). The CX pathway is highly conserved across insects and has been shown to integrate skylight cues such as polarized light and the sun in the brains of locusts (Heinze, 2014;

Homberg, 2004; Homberg, Heinze, Pfeiffer, Kinoshita, & el Jundi, 2011; Homberg, Hofer, Pfeiffer, & Gebhardt, 2003), fruit flies (Sancer et al., 2019; Warren, Giraldo, & Dickinson, 2019), dung beetles (el Jundi, Warrant, Pfeiffer, & Dacke, 2018; Immonen, Dacke, Heinze, & el Jundi, 2017), monarch butterflies (Heinze, Florman, Asokaraj, el Jundi, & Reppert, 2013; Heinze & Reppert, 2011), several bee species (Held et al., 2016; Pfeiffer & Kinoshita, 2012; Stone et al., 2017; Zeller et al., 2015), and *Cataglyphis* ants (Grob, Fleischmann, Grübel, Wehner, & Rössler, 2017; Schmitt, Stieb, Wehner, & Rössler, 2016). In all insects investigated so far, sky-compass information is received by photoreceptors in the compound eyes and transmitted from the medulla (ME) of the optic lobe (OL) via the anterior optic tract (AOT) to the anterior optic tubercle (AOTU). Further neuronal projections connect the AOTU to the lateral complex (LX) and, from there, to the CX. The CX integrates different celestial cues (el Jundi, Pfeiffer, Heinze, & Homberg, 2014; Heinze & Homberg, 2007; Homberg et al., 2011) with other sensory information and represents a high-order center for motor control in insects (Guo & Ritzmann, 2013; Martin, Guo, Mu, Harley, & Ritzmann, 2015; Seelig & Jayaraman, 2015; Strauss, 2002). The second pathway to the MB transmits the visual information to be processed in many parallel microcircuits involved in learning and memory formation (for reviews, see Heisenberg, 2003; Menzel, 2014) as well as multisensory integration of stimuli (Kirkhart & Scott, 2015; Lin, Lai, Chin, Chen, & Chiang, 2007; Liu, Wolf, Ernst, & Heisenberg, 1999). As a special feature in Hymenoptera, projection neurons of the ME form a prominent anterior superior optic tract (ASOT) that projects to the collar (CO) region of the MB calyces in both hemispheres of ants (Ehmer & Gronenberg, 2004; Grob et al., 2017; Gronenberg, 1999, 2001; Yilmaz et al., 2016) and bees (Ehmer & Gronenberg, 2002; Gronenberg, 2001; Mobbs, 1984).

Most previous studies focused on these two visual pathways, while a comprehensive description of further visual tracts, their target neuropils in the central brain, and physiological relevance are largely missing in Hymenoptera. The reason for this, most likely, is because many of their target regions in the cerebrum, an area termed central adjoining neuropil (CANP), lack clear boundaries between the enclosed individual neuropil regions. Although the neuropils of the CANP have gained less attention, they probably play as much a role in the processing of visual information as the previously established neuropils, such as the AOTU, MB, or CX. For a similar reason, and to be able to assign other attributes to distinct brain regions, a consortium of insect neuroanatomists introduced a systematic nomenclature for all neuropils and fiber tracts of the insect brain using *Drosophila* as a model insect (Ito et al., 2014). Further studies created 3D maps of the brains of the monarch butterfly (Heinze & Reppert, 2012), the ant *Cardiocondyla obscurior* (Bressan et al., 2015), the dung beetle *Scarabaeus*

lamarcki (Immonen et al., 2017), and, more recently, the desert locust *Schistocerca gregaria* (von Hadeln, Althaus, Häger, & Homberg, 2018).

In this study, we provide a comprehensive map of synapse-rich neuropils and major connecting fiber tracts including all visual pathways in the brain of the thermophilic ant *Cataglyphis nodus*. By means of immunohistochemical staining and anterograde fluorescent tracing, we were able to define and reconstruct 25 paired and 8 unpaired synapse-rich neuropils and found an overall number of 30 connecting fiber tracts. We further labeled and described six major optical tracts and commissures and their projections into the central brain. This extensive neuronal circuitry demonstrates the complexity of the visual system of *Cataglyphis* ants and emphasizes the importance of further studies to understand the complex processing of visual navigational information in the insect brain.

2 | MATERIAL AND METHODS

2.1 | Animals

Cataglyphis nodus colonies were collected at Schinias National Park, Greece (38°80′N, 24°01′E), and Strofylia National Park, Greece (38°15′N, 21°37′E), and transferred to Würzburg. The ants were kept under a 12 hr/12 hr day/night cycle in a climate chamber with constant temperature (24°C) and humidity (30%). The animals had permanent access to water and were fed with honey water (1:2) and dead cockroaches twice per week. For all neuroanatomical studies, *Cataglyphis* workers of unknown age and previous experiences were randomly chosen from queenless colonies.

Please note that in some previous publications, the species name *Cataglyphis nodus* was *Cataglyphis noda*, to match the species with the feminine gender of the genus (for details see Rössler, 2019). As the term *nodus* (latin) is a masculine noun, it should stay unchanged, in opposition to the name of the genus. This is in accordance with Articles 11.9.1.2 and 34.2.1 of the International Code of Zoological Nomenclature of 1999 (B. Bolton, pers. comm.). We therefore use *C. nodus*, as suggested in Rössler (2019).

2.2 | Antibody characterization

To visualize the synaptic neuropils and fiber tracts in *Cataglyphis*, we used a monoclonal antibody to synapsin (SYN-ORF1, mouse@synapsin; kindly provided by E. Buchner and C. Wegener, University of Würzburg, Germany) and fluorescently labeled Alexa Fluor® 488-phalloidin (Invitrogen, Carlsbad, CA; Cat# A12379). The presence of synapsin in presynaptic terminals is highly conserved among invertebrates (Hofbauer et al., 2009; Klagges et al., 1996). The specificity of the antibody has been characterized in *Drosophila* (Klagges et al., 1996) and in the honey bee *Apis mellifera* (Pasch, Muenz, & Rössler, 2011) and its affinity was confirmed in numerous neuroanatomical studies on diverse insect species (Groh & Rössler, 2011; Immonen et al., 2017; von Hadeln et al., 2018)

including *Cataglyphis* ants (Schmitt, Stieb, et al., 2016; Schmitt, Vanselow, Schlosser, Wegener, & Rössler, 2016; Stieb, Hellwig, Wehner, & Rössler, 2012; Stieb, Muenz, Wehner, & Rössler, 2010). Phalloidin is a cyclic peptide originating from the fungus *Amanita phalloides*, which binds to filamentous actin, for example, in dendritic tips (Dancker, Low, Hasselbach, & Wieland, 1975; Frambach, Rössler, Winkler, & Schürmann, 2004), and axonal processes (Rössler, Kuduz, Schürmann, & Schild, 2002). It has recently been used to study brain structures in *Cataglyphis* (Schmitt, Stieb, et al., 2016; Stieb et al., 2010). The combination of fluorescently labeled phalloidin and anti-synapsin increased the contrast of tissue structures and, thus, allowed for a more accurate demarcation of the borders within the CANP.

For additional information about the neuropil boundaries and substructures, we used a polyclonal anti-serotonin antibody (rabbit@5-HT; Immunostar, Hudson, WI; Cat# 20080). The specificity of the anti-serotonin antibody was previously tested in dung beetles (Immonen et al., 2017) and its functionality has been demonstrated in diverse insect species (Dacks, Christensen, & Hildebrand, 2006; Falibene, Rössler, & Josens, 2012; Hoyer, Liebig, & Rössler, 2005; Watanabe, Shimohigashi, & Yokohari, 2014; Zieger, Bräunig, & Harzsch, 2013). We used Alexa Fluor® 568-goat@rabbit (Molecular Probes, Eugene, OR; Cat# A11011) and CF633 goat@mouse (Biotium, Hayward, CA; Cat# 20121) as fluorescently labeled secondary antibodies.

2.3 | Immunohistochemistry

Ants were anesthetized on ice before the head was cutoff and fixed in dental wax coated dishes. A small window was cut between the compound eyes of the head, and the brain tissue was dissected out and covered in ice-cold ant ringer saline (127 mM NaCl, 7 mM KCl, 2 mM CaCl2, 7.7 M Na2HPO4, 3.8 M KH2PO4, 4 mM TES, and 3.5 mM trehalose; pH 7.0). For whole-mount staining, the brains were fixed in 4% formaldehyde (FA) in phosphate-buffered saline (PBS) overnight at 4°C. Brains were washed in PBS (3 × 10 min) on the next day and afterward treated with PBS containing Triton-X (2% PBST for 10 min, 0.2% PBST for 2 × 10 min) to facilitate the penetration of the antibodies. After pre-incubation with 2% normal goat serum (NGS) in 0.2% PBST (4°C, overnight), samples were incubated in the primary antibody solution (1:50 anti-synapsin, 2% NGS in 0.2% PBST) for 4 days at 4°C (Table 1). They were rinsed in PBS (3 × 20 min) followed by an incubation in the primary polyclonal antiserum against 5-HT (1:4000 anti-5-HT, 1% NGS in 0.2% PBST) for another 4 days at 4°C. Subsequently, the brains were incubated in the secondary antibody solution (1:250) and phalloidin (1:200) combined with 1% NGS in PBS for 3 days at 4°C. The brains were then washed in PBS (4 × 20 min) and post-fixed overnight in 4% FA in PBS at 4°C. After rinsing with PBS, the samples were dehydrated in an ethanol series (30, 50, 70, 90, 95, 100, and 100% for 3–4 min each step), cleared in methyl salicylate (35 min; M-2047; Sigma Aldrich, Steinheim, Germany) and mounted in Permount (Fisher Scientific, Schwerte, Germany; Cat# 15820100).

TABLE 1 Primary antibodies

Antibody	Immunogen	Manufacturer; species; clonality; Cat #; RRID	Dilution
Synapsin	*Drosophila* Synapsin glutathione-S-transferase fusion protein	E. Buchner, Theodor-Boveri-Institute, University of Würzburg, Germany; mouse; monoclonal; Cat # 3C11 (SYNORF1); RRID: AB_528479	1:50
Serotonin (5-HT)	5-HT coupled to bovine serum albumin with paraformaldehyde	Immunostar, Hudson, WI; rabbit; polyclonal; Cat # 20080; RRID: AB_572263	1:4,000

2.4 | Neuronal tracing

All neuronal tracings were done by using combinations of tetramethylrhodamine-biotin dextran (Microruby, 3,000 MW, lysine fixable; Molecular Probes, Eugene, OR, D-7162) and Alexa Fluor 488 dextran (10,000 MW, lysine fixable; Molecular Probes, Eugene, OR, D-22910). To trace the visual and olfactory tracts, the animals were anesthetized on ice, mounted on a holder and the head and antennae were fixed by using dental wax. A square window was cut into the head capsule, and trachea and glands were removed. Subsequently, the brain was rinsed with ant ringer saline before the fluorescent tracer was injected with a glass capillary into the neuropil of interest. To distinguish between tracts that were stained through injections into the ME and lobula (LO) of the same OL, different fluorescent tracers were used. In addition, the olfactory tracts were analyzed in a different set of brain samples by injecting Microruby into the antennal lobes (ALs). After injection, the injection site was rinsed in ant ringer saline and the head capsule was resealed to avoid dehydration of the brain. For anterograde staining of the antennal nerves (ANs), the antennae were cut close to their base and Microruby was added on the antennae stump. In all cases, the animals were stored in humidified chambers in the darkness for 5 hr to allow the dye to be transported. The brains were afterward dissected and fixated in 4% FA in PBS overnight at 4°C. To visualize the neuropils that are innervated by the visual tracts, the corresponding brains were additionally incubated with anti-synapsin antibody as described above. Finally, all brains were rinsed in PBS (5 × 10 min), dehydrated in an ethanol series (30, 50, 70, 90, 95, 100, 100, and 100%; each step 10 min), cleared in methyl salicylate (35 min), and embedded in Permount.

2.5 | Laser scanning confocal microscopy and image processing

Brain samples were scanned with a confocal laser scanning microscope (either Leica TCS SP2 or Leica TCS SP8, Leica Microsystems AG, Wetzlar, Germany) using a 20× water immersion objective (20.0 × 0.7/0.75 NA). The fluorophores were excited with a wavelength of 488 nm for phalloidin and Alexa Fluor 488 dextran, 568 nm for anti-5-HT and Microruby, and 633 nm for anti-synapsin. All samples were scanned at a step size of 4–6 μm in z-direction and at a resolution of 1,024 × 1,024 pixels in xy-direction. Image stacks were processed using ImageJ (ImageJ 1.52p; Wayne Rasband, NIH, Bethesda, MD) and CorelDRAW X8 (Version 20.1.0.708, Corel Corporation, Ottawa, ON, Canada). If necessary, contrast was adjusted in ImageJ. Pairwise 2D-stitching was performed with the stitching plugin in ImageJ (Preibisch, Saalfeld, & Tomancak, 2009).

2.6 | 3D reconstruction and labeling

Three-dimensional (3D) reconstructions of neuropils and fiber tracts were based on anti-synapsin, anti-5-HT, and phalloidin labeling using the software Amira 2019.1 (FEI, Visualization Sciences Group; Hillsboro, OR; http://thermofisher.com/amira-avizo). In anti-synapsin staining, only synapse-rich regions are stained while most fiber bundles appear as dark regions. On the other hand, phalloidin staining highlights differences of f-actin distributions between fiber tracts and neuropils. The combination of both techniques in whole-mount brains enabled us to better visualize the contours of individual fiber tracts and neuropils. Voxels of the structures of interest were manually labeled in two dimensions in the segmentation editor and, afterward, interpolated using the interpolation tool. The interpolated contours were double checked and manually corrected in case of deviations from the gray values of the image stack. The corresponding 3D models were generated using the SurfaceGen module.

We followed the unified nomenclature for insect brain introduced by Ito et al. (2014) to define known neuropils and fiber tracts. For undescribed structures, we introduced new terms while accurately following the general rules of the nomenclature (Ito et al., 2014). To define the borders of the brain regions of the CANPs, clearly identifiable fiber tracts and neuropils were used as landmarks. In addition, visible structural alterations of the brain tissue and/or serotonergic innervation patterns were used to discriminate between individual neuropils, similar to the technique introduced by Immonen et al. (2017) and Heinze and Reppert (2012). In some cases, no apparent distinction between neuropils was possible. In these cases, the borders were defined based on traceable and reproducible landmark criteria.

The orientation of the *Cataglyphis* brain relative to its body axis is tilted by about 90° in comparison to that of, for example, *Drosophila* (Ito et al., 2014; Pereanu, Kumar, Jennett, Reichert, & Hartenstein, 2010). Consequently, anterior in *Drosophila* appears as dorsal in *Cataglyphis*, posterior as ventral. As the different orientation can be misleading in comparison with other insect brains, this should be kept in mind, especially considering the nomenclature of individual neuropils and their position in the brain (e.g., the superior neuropils [SNPs] are in the anterior brain region in *Cataglyphis*).

3 | RESULTS

3.1 | General layout of the *Cataglyphis* brain

The central brain of Hymenoptera is organized bilaterally, and the protocerebrum, deutocerebrum, and tritocerebrum are fused into one cerebral ganglion (CRG) with less distinct borders (Dettner & Peters, 2011). In *Cataglyphis*, the CRG on its two lateral ends is enclosed by (compared to many other ant species) relatively large OLs (Figure 1a–d,f,g). The distal regions of the OLs are directly attached to the compound eye's retina. The most conspicuous structures of the CRG are the calyces (CAs) of the MBs, which are located at the dorsal tip of the brain
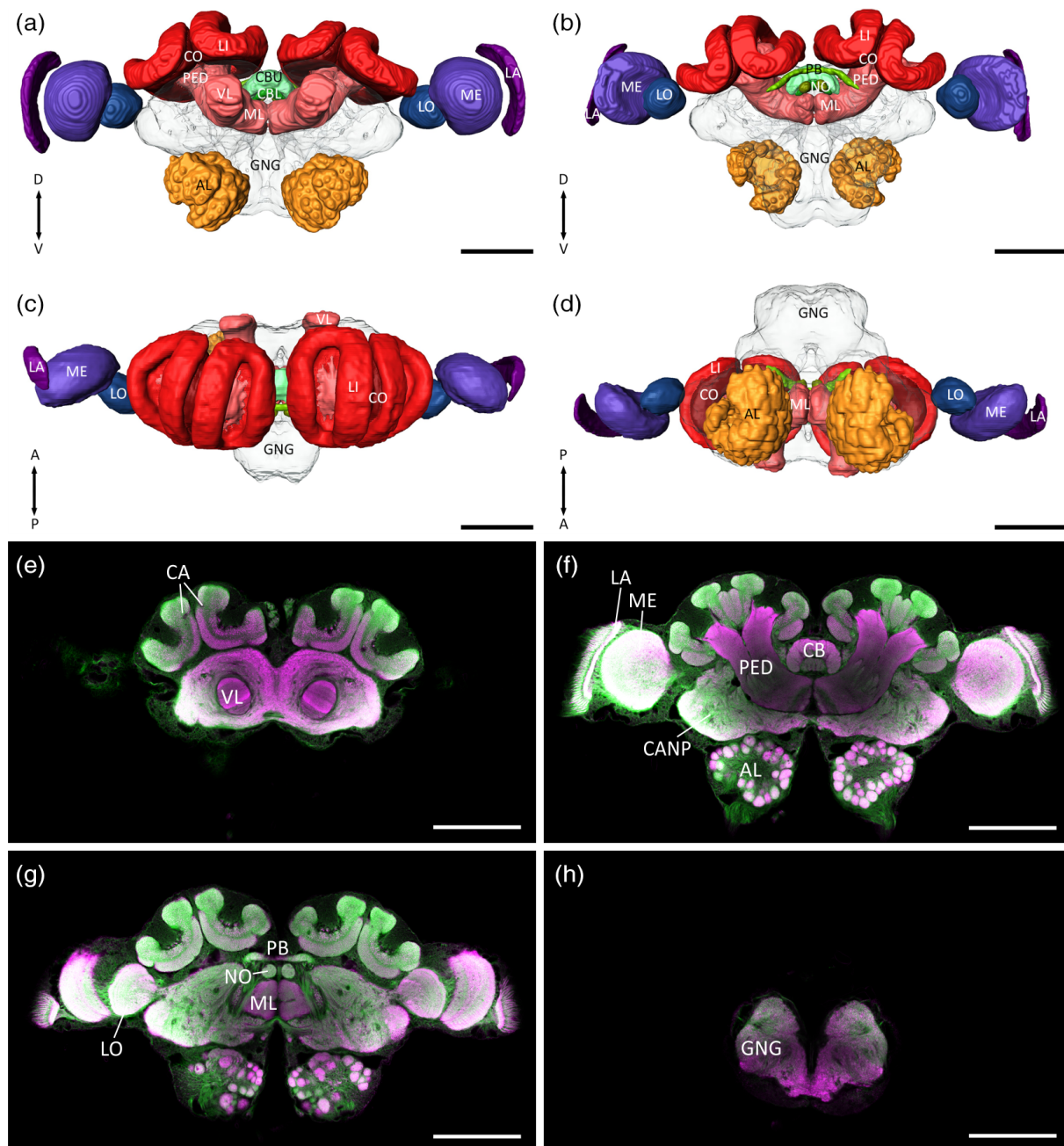
FIGURE 1 General layout of the *Cataglyphis nodus* brain. (a–d) Surface reconstructions of the well-defined brain neuropils include the antennal lobes (ALs), the mushroom bodies (MBs), the optic lobes (OLs), and the central complex (CX). The reconstruction of the neuropils is visualized from different views: (a) anterior, (b) posterior, (c) dorsal, and (d) ventral. The MB can be further subdivided into the calyces (CA), which comprise the collar (CO) and lip (LI), the pedunculus (PED), and the medial and vertical lobes (ML and VL). The CX consists of the central body (CB), the protocerebral bridge (PB), and the noduli (NO), and the optic lobes comprise the lamina (LA), medulla (ME), and lobula (LO). The central adjoining neuropils (CANP, gray) and the gnathal ganglion (GNG, green) are shown as transparent structures. (e–h) Examples of confocal images from anterior (e) to posterior (h) of the whole brain. The preparation was double-stained with anti-synapsin (magenta) and phalloidin (green) to ensure the highest contrast of the fiber bundles and neuropils. Scale bars = 200 μm [Color figure can be viewed at wileyonlinelibrary.com]
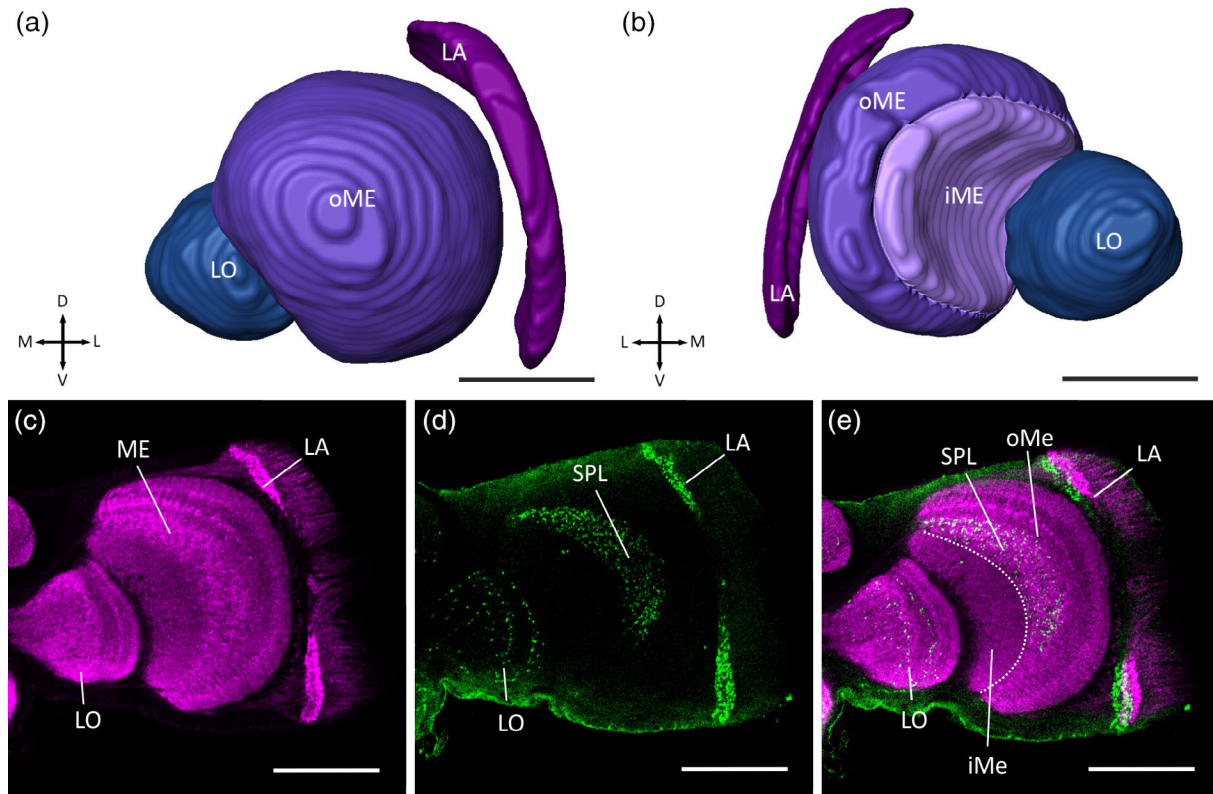
FIGURE 2 The optic lobes of *Cataglyphis nodus*. (a, b) Three-dimensional reconstruction of the optic lobes. The optic lobes consist of the lamina (LA), medulla (ME), and lobula (LO). The medulla can be further subdivided into an inner (iME) and outer medulla (oME): (a) anterior view and (b) posterior view. (c–e) Confocal images of the optic lobes based on anti-synapsin (c, magenta), anti-serotonin (d, green) labeling, or both (e). The serpentine layer (SPL) demarcates the border between iME and oME. Scale bars = 100 μm [Color figure can be viewed at wileyonlinelibrary.com]

(Figure 1a–c,e–g). The ALs contain olfactory glomeruli (Figure 1f,g) and extend to the most ventral regions of the CRG. As in all hymenopteran species (Dettner & Peters, 2011), the gnathal ganglion (GNG) is fused ventrally to the CRG and demarcates the posterior end of the central brain (Figure 1a–d,h). In insects, the GNG comprises three neuromeres: the mandibular, maxillary and labial ganglia, which are fused into one brain region (Scholtz & Edgecombe, 2006). Several neuropils of the central brain are surrounded by glial cells and, thus, exhibit well-defined boundaries. This applies to the ALs, the neuropils of the CX, the MBs, and the neuropils of the OLs—and is consistent with anatomical studies in other insects (Adden, Wibrand, Pfeiffer, Warrant, & Heinze, 2020; Brandt et al., 2005; Bressan et al., 2015; el Jundi, Huetteroth, Kurylas, & Schachtner, 2009; Groothuis, Pfeiffer, el Jundi, & Smid, 2019; Heinze & Reppert, 2012; Immonen et al., 2017; Ito et al., 2014; von Hadeln et al., 2018). The general shape and structural characteristics of these neuropils in the brain of *Cataglyphis nodus* are also similar to the findings in the honey bee (Brandt et al., 2005). The MB and the CX are surrounded by the CANP, which make up a considerable proportion of the *Cataglyphis* brain (Figure 1e–g).

3.2 | Sensory input regions

In contrast to the majority of ant species (Gronenberg, 2008), the OLs represent the largest sensory input area in the brain of *Cataglyphis*

(Figure 1). They serve as primary processing centers before the visual information is transferred via projection neurons to high-order processing and integration sites (reviewed by Rössler, 2019). From distal to medial, the OLs consist of the lamina (LA), the ME, and the LO (Figure 2a–c). Based on anti-synapsin and 5-HT staining, the ME can be further subdivided into the inner medulla (iME) and outer medulla (oME). A relatively prominent layer of serotonergic processes demarcates the proximal boundary between the oME and iME (Figure 2d,e). Although tracings indicate that visual information from the dorsal rim area is transmitted via separate paths along dorsal parts of the LA and ME (Grob et al., 2017), no structural features of a distinct dorsal rim area can be localized within the ME or the LA, unlike to what has been shown in some other insects (el Jundi, Pfeiffer, & Homberg, 2011; Pfeiffer & Kinoshita, 2012; Schmeling, Tegtmeier, Kinoshita, & Homberg, 2015; Zeller et al., 2015).

The ALs process the olfactory information from olfactory receptor neurons (ORNs) housed in sensilla on the insect antenna. ORN axons project into the glomeruli of the AL. The ALs of *Cataglyphis nodus* contain around 226 olfactory glomeruli (Figure 1a,b,d,f,g) (for glomerulus numbers, see Stieb, Kelber, Wehner, & Rössler, 2011).

3.3 | High-order processing centers

The MBs are very prominent neuropils in the *Cataglyphis* central brain (Figure 1). The neuroanatomy of the MBs is typical for

Aculeata: each MB consists of a cup-shaped medial and lateral calyx (MCA and LCA), a pedunculus (PED), as well as a medial lobe (ML) and a vertical lobe (VL) (Figures 1 and 3). The MCA and LCA form major input regions of the MB and receive olfactory as well as visual information from afferent projection neurons of the primary sensory neuropils. In *Cataglyphis* each calyx can be subdivided into two subneuropils: the lip (LI) and collar (CO) (Figure 3a,b,d–g). Both LI and CO exhibit characteristic microglomerular structures (Figure 3e–g). Numerous microglomeruli in the visual (LI) and

olfactory (CO) subregions of the MB calyx provide thousands of parallel microcircuits forming a rich neuronal substrate for memory formation (Stieb et al., 2012; for reviews, see Rössler, 2019; Groh & Rössler, 2020). In comparison to many other (mostly olfactory guided) ant species (Gronenberg, 1999, 2001), the visual CO is relatively prominent in the *Cataglyphis* MB (Figure 3d–g), further supporting the prominent role of vision. The axons of MB intrinsic neurons (Kenyon cells [KCs]) innervate the PED and terminate in the ML and VL (Figure 3a,b,d,e–g), which are the major output regions
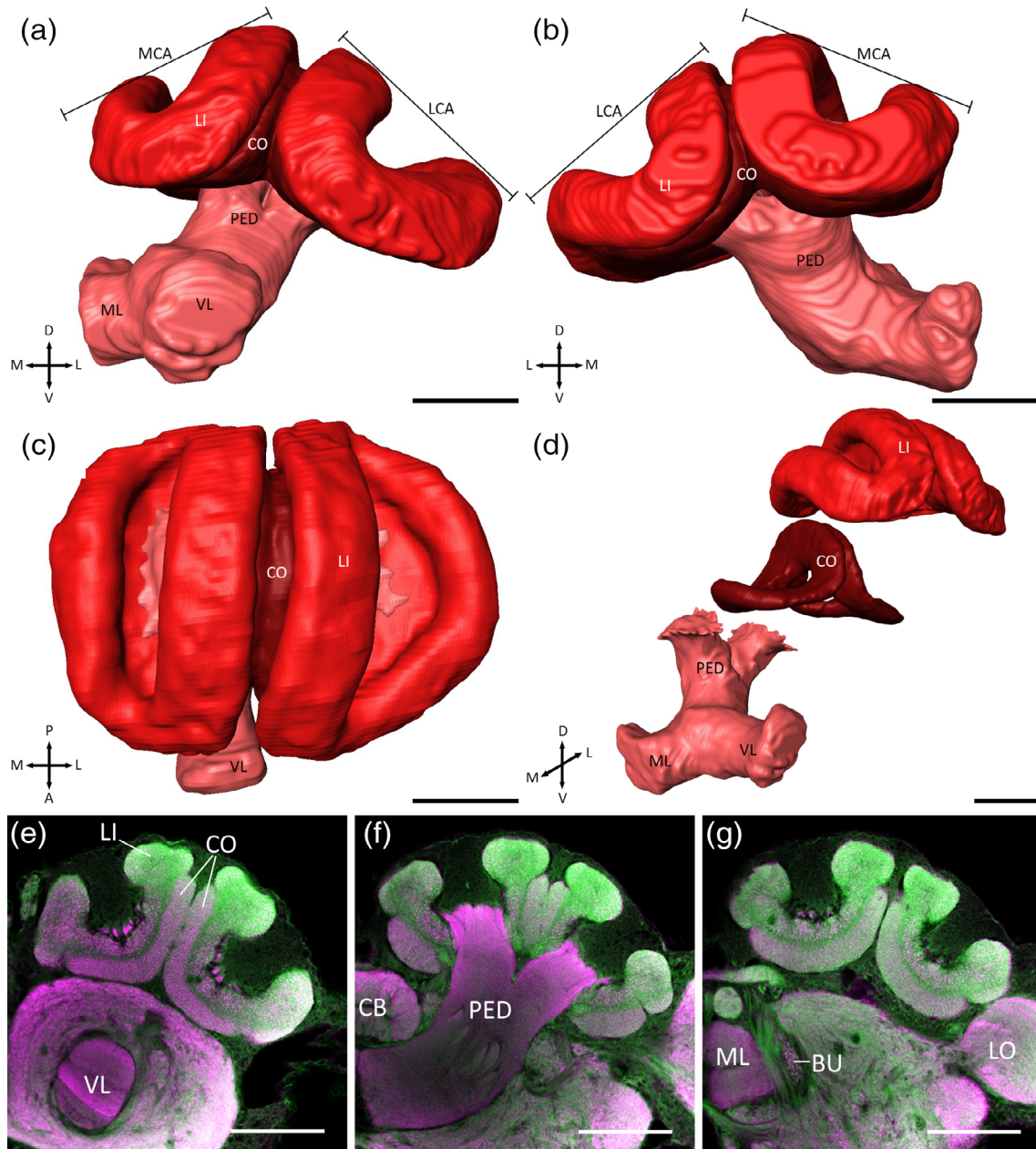
FIGURE 3 The mushroom body (MB) of *Cataglyphis nodus*. The MB consists of the pedunculus (PED), medial and vertical lobes (ML and VL), and the medial and lateral calyces (MCA and LCA). The calyces can be further subdivided into collar (CO) and lip (LI). (a–d) Three-dimensional reconstruction of the MB. (a) Anterior view, (b) posterior view, (c) dorsal view, and (d) oblique anteromedial view of the distinct neuropils of the MB. (e–g) Confocal images of the MB from anterior (e) to posterior (g) of a whole-mount preparation (anti-synapsin: magenta; phalloidin: green). Scale bars = 100 μm. BU, bulb; LO, lobula [Color figure can be viewed at wileyonlinelibrary.com]

of the MBs (Farris, 2005; Li & Strausfeld, 1997; Strausfeld, Homburg, & Kloppenberg, 2000; Strausfeld, Sinakevitch, Brown, & Farris, 2009). In *Cataglyphis*, the ML is in the inferior region of the brain, ventral to the CX (Figure 3f,g), while the VL extends in a perpendicular angle toward the anterior brain surface and forms, together with SNPs, the anteriormost structures of the brain (Figure 3a,d,e). On its lateral side, the VL is connected to the calyces by the protocerebral-calycal tract (PCT), which represents an intrinsic feedback circuit of the MB (Figure 5a,e). GABAergic PCT-neurons have been characterized most extensively in honey bees (Grünewald, 1999; Haehnel & Menzel, 2010; Mobbs, 1982) and may be a general feature of hymenopteran MBs.

Sky-compass information converges in the CX before being passed on to premotor centers (Schmitt, Stieb, et al., 2016; Grob et al., 2017; reviewed by: Rössler, 2019). As in other insects, the CX is positioned at the brain midline (Figure 1). It is composed of four distinct neuropils: the upper (CBU) and lower division (CBL) of the central body (CB), the paired noduli (NO), and the protocerebral bridge (PB) (Figure 4). The CBU is often referred to as the fan-shaped body and the CBL as ellipsoid body. The anteriormost neuropil of the CX is the CBU. To its posterior end, it mounts dorsally on top of the CBL. Both neuropils are located medial to the pedunculi and superior to the MLs of the MBs (Figure 7e–h). More posterior in the brain lies the PB (Figure 7i–k). The only paired structures of the CX in ants are the NO (Figures 4b,d, and 7i).

3.4 | Central adjoining neuropils

In contrast to the major neuropils, the individual regions within the CANP are mostly unsheathed by glial processes and possess less distinct borders in the insect brain (Ito et al., 2014). To define neuropil boundaries, we used prominent fiber bundles as discernable landmarks, as it has also been done in previous work on other insects (Heinze & Reppert, 2012; Immonen et al., 2017; von Hadeln et al., 2018). We first localized and reconstructed the fiber tracts in the *Cataglyphis* brain (Figure 5) to further determine the ambiguous areas of the CANP. The output pathways of the ALs have been studied in detail, in particular in honey bees and are described as a dual olfactory pathway (Kirschner et al., 2006; reviewed by: Galizia & Rössler, 2010; Rössler & Brill, 2013). In *Cataglyphis*, we found five output tracts, termed antennal lobe tracts (ALTs), which transfer the olfactory information via projection neurons to higher brain regions: the medial (m-ALT), the lateral (l-ALT), and three mediolateral tracts (ml-ALT; Figure 6a). The ml-ALTs are considerably thinner and extend their arborizations into some CANP: the ventrolateral neuropils (VLNP), the superior intermediate protocerebrum (SIP) and the lateral horn (LH, Figure 6a,c). In contrast, the m-ALT and the l-ALT are two of the largest fiber bundles in the entire brain. Both tracts project into the ipsilateral LI and LH (Figure 6a, b). While the m-ALT first passes through the LI of the CA (and afterward into the LH), the l-ALT enters the LH first (Figure 6a,b), similar to the findings in the honey bee and in *Camponotus floridanus* (Kirschner et al., 2006; Zube, Kleineidam, Kirschner, Neef, & Rössler, 2008).
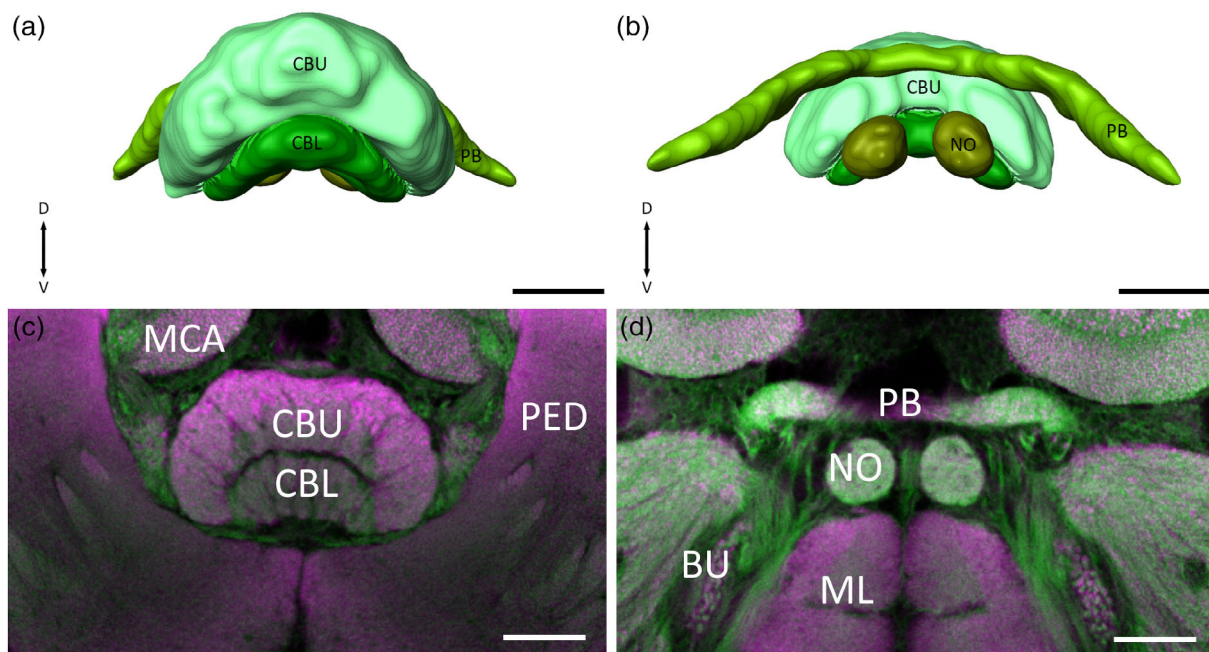
FIGURE 4 The central complex (CX) of *Cataglyphis nodus*. The CX consists of the upper (CBU) and lower divisions (CBL) of the central body, the protocerebral bridge (PB), and the paired noduli (NO). (a, b) Three-dimensional reconstructions of the central complex: (a) anterior view and (b) posterior view. (c, d) Confocal images of the CX from anterior (c) to posterior (d) in a whole-mount preparation. The preparation was double-stained with anti-synapsin (magenta) and phalloidin (green). Scale bars = 50 μm. BU, bulb; MCA, medial calyx; ML, medial lobe; PED, pedunculus [Color figure can be viewed at wileyonlinelibrary.com]
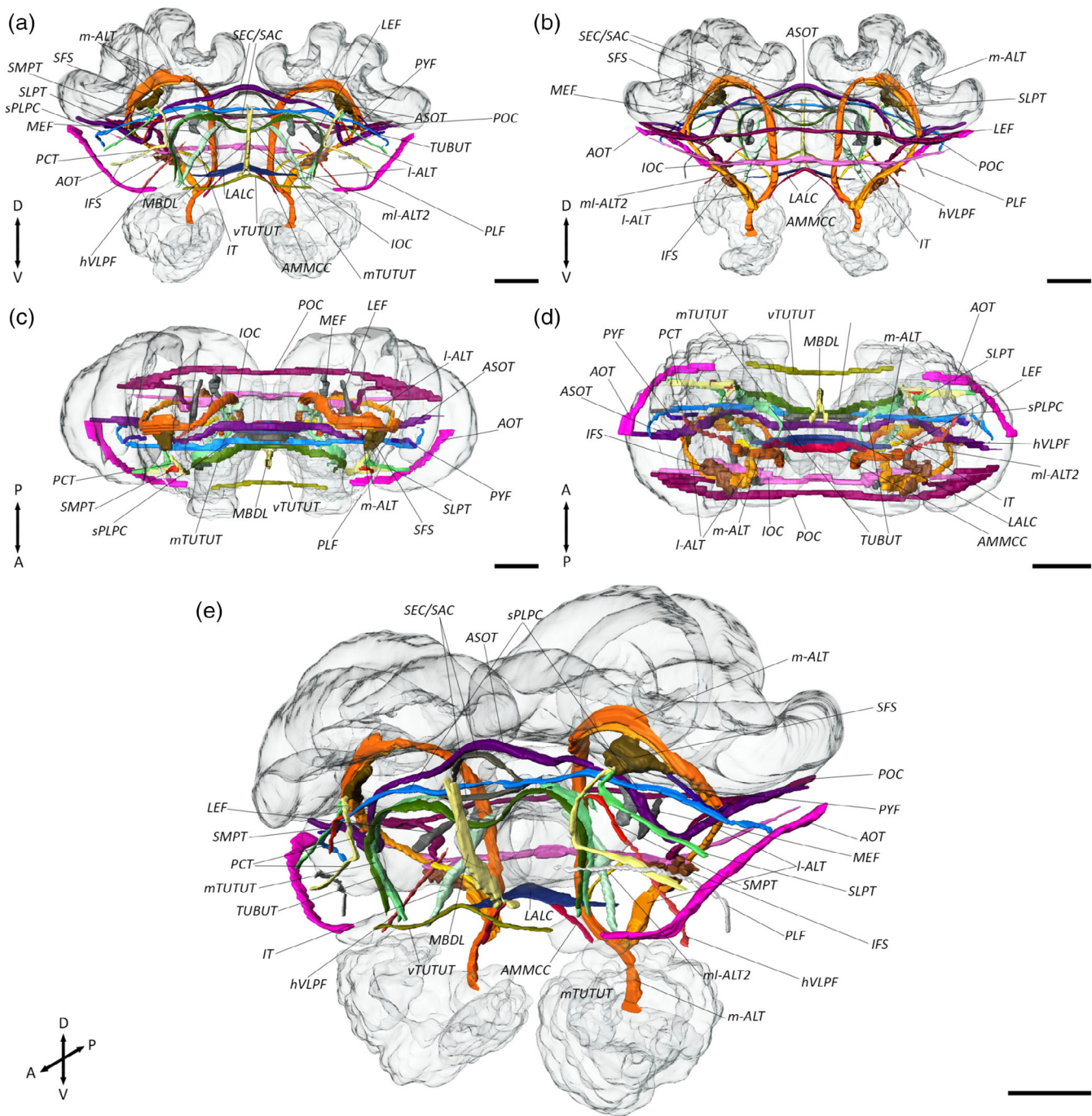
FIGURE 5 Three-dimensional reconstruction of important fiber bundles in the *Cataglyphis nodus* brain. Only tracts and commissures that could be clearly localized and identified based on anti-synapsin and f-actin phalloidin staining were reconstructed. The mushroom bodies, the central complex, and the antennal lobes are shown in transparent. (a) Anterior view; (b) posterior view; (c) dorsal view; (d) ventral view; (e) oblique anterolateral view. Scale bars = 100 μm. AMMCC, antennal mechanosensory and motor center commissure; AOT, anterior optic tract; ASOT, anterior superior optic tract; hVLPF, horizontal ventrolateral protocerebrum fascicle; IFS, inferior fiber system; IOC, inferior optic commissure; IT, isthmus tract; LALC, lateral accessory lobe commissure; l-ALT, lateral antennal lobe tract; LEF, lateral equatorial fascicle; m-ALT, medial antennal lobe tract; MBDL, median bundle; MEF, medial equatorial fascicle; ml-ALT, mediolateral antennal lobe tract; mTUTUT medial tubercle-tubercle tract; PCT, protocerebral-calycal tract; PLF, posterior lateral fascicle; POC, posterior optic commissure; PYF, pyriform fascicle; SEC/SAC, superior ellipsoid/arch commissure; SFS, superior fiber system; SLPT, superior lateral protocerebrum tract; SMPT, superior medial protocerebrum tract; sPLPC, superior posterolateral protocerebrum commissure; TUBUT, tubercle-bulb tract; vTUTUT, ventral tubercle-tubercle tract [Color figure can be viewed at wileyonlinelibrary.com]
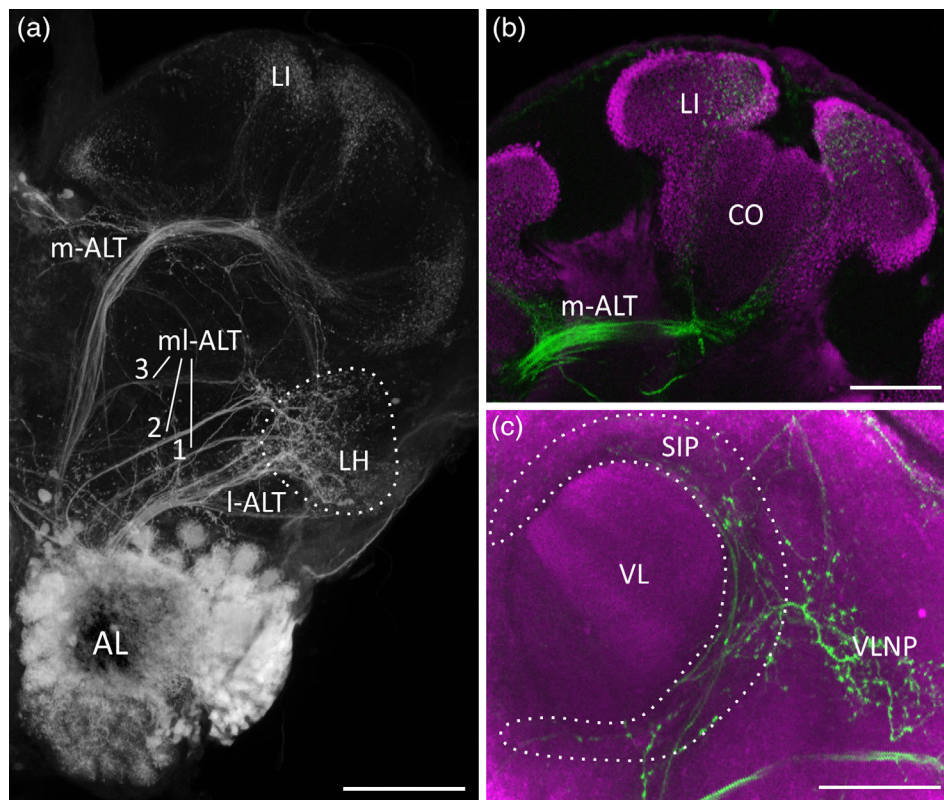
FIGURE 6 Projections from the antennal lobes (ALs) into the central brain. Anterograde staining was obtained by microruby injections (gray/green) into the AL. The pre-synapses are visualized with anti-synapsin labeling (magenta; b, c). (a) Overview of the antennal lobe tracts. The medial antennal lobe tract (m-ALT) and lateral antennal lobe tract (l-ALT) project into the lateral horn (LH) and the lip (LI) of the mushroom body (MB). The mediolateral antennal lobe tracts (ml-ALT) 1–3 project into different parts of the central adjoining neuropils including the LH. Z-projection from a stack of 27 images with 5 μm step size. (b) Projections of the ALTs into the LI. Z-projection from a stack of seven images with 5 μm step size. (c) Projections of the ALTs into the ventrolateral neuropils and the superior intermediate protocerebrum. Z-projection from a stack of 11 images with 5 μm step size. Scale bars = 100 μm (a) and 50 μm (b, c) [Color figure can be viewed at wileyonlinelibrary.com]

With the help of these tracts as crucial landmarks, the CANP can be subdivided in different brain regions that include the AOTU, the LX, the SNP, the inferior neuropils (INP), the ventromedial neuropils (VMNP), the LH, the VLNP, and the periesophageal neuropils (PENP). Overall, we defined 15 paired and 5 unpaired neuropils in the central adjoining brain region (Figures 7 and 8).

3.5 | Anterior optic tubercle

The AOTU is an important high-order visual processing center in insects. As demonstrated in previous studies on locusts, butterflies and honey bees, the AOTU is involved in processing polarized-light information (el Jundi & Homberg, 2012; Heinze & Reppert, 2011; Pfeiffer, Kinoshita, & Homberg, 2005) and chromatic cues (Kinoshita, Pfeiffer, & Homberg, 2007; Mota, Gronenberg, Giurfa, & Sandoz, 2013; Pfeiffer & Homberg, 2007). In *Cataglyphis*, the AOTU is located superficially in the ventrolateral brain region (Figures 7a,b and 8a) and can be subdivided into two compartments: the upper and the lower subunits (Figure 9a). Projection neurons of the tubercle-bulb tract (TUBUT) transmit the visual information from the AOTU to the ipsilateral bulb

(BU, Figure 9a). Before the axons finally terminate in the BU, they project around the VL superiorly and pass by the SIP, the antler (ATL), and the clamp (CL). In addition, the AOTUs of both hemispheres are interconnected by the medial tubercle-tubercle tract (mTUTUT) and the ventral tubercle-tubercle tract (vTUTUT, Figure 9a). The mTUTUT neurons originate from the TUBUT. After passing the VL, they bifurcate from the TUBUT and cross the midline through the ATL, anteroventral to the CBU. In contrast to the mTUTUT neurons, the vTUTUT neurons connect the upper subunits along an almost straight course at the inferiormost border of the superior medial protocerebrum (SMP). Similar intertubercle tracts have been previously described in honey bees (Mota, Yamagata, Giurfa, Gronenberg, & Sandoz, 2011), bumblebees (Pfeiffer & Kinoshita, 2012), and locusts (el Jundi et al., 2011; el Jundi & Homberg, 2012; Pfeiffer et al., 2005), implying a general characteristic of the interconnection of the AOTUs.

3.6 | Lateral complex

The LX consists of the lateral accessory lobe (LAL) and the bulb (BU) in *Cataglyphis*. The BU is recognizable by its very large
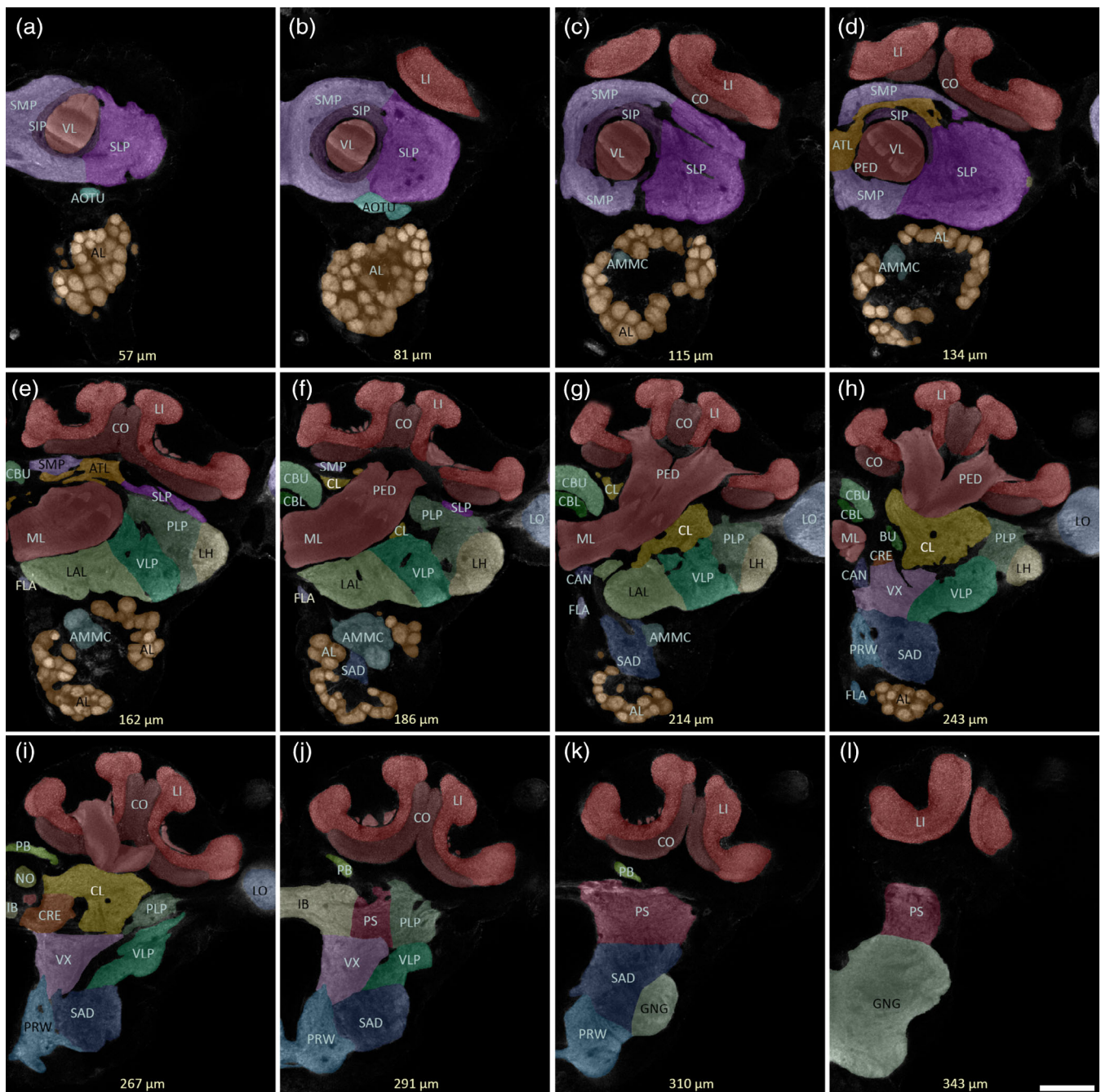
FIGURE 7 Confocal images (anterior view) of the neuropils of the central brain of *Cataglyphis nodus*. The optical sections (anti-synapsin staining) are shown from anterior (a) to posterior (l). Individual neuropils were labeled with transparent colors to demarcate their boundaries. Scale bar = 100 μm. AL, antennal lobe; AMMC, antennal mechanosensory and motor center; AOTU, anterior optic tubercle; ATL, antler; BU, bulb; CAN, cantle; CBL, central body lower division; CBU, central body upper division; CL, clamp; CO, collar; CRE, crepine; FLA, flange; GNG, gnathal ganglion; IB, inferior bridge; LAL, lateral accessory lobe; LH, lateral horn; LI, lip; LO, lobula; ML, medial lobe; NO, noduli; PB, protocerebral bridge; PED, pedunculus; PLP, posterolateral protocerebrum; PRW, prow; PS, posterior slope; SAD, saddle; SIP, superior intermediate protocerebrum; SLP, superior lateral protocerebrum; SMP, superior medial protocerebrum; VL, vertical lobe; VLP ventrolateral protocerebrum; VX, ventral complex [Color figure can be viewed at wileyonlinelibrary.com]

microglomerular synaptic structures (Figures 3g and 4d) and presents a prominent synaptic relay of the sky-compass pathway (el Jundi et al., 2018; Grob et al., 2017; Heinze & Reppert, 2011; Held et al., 2016; Homberg et al., 2003; Pfeiffer & Kinoshita, 2012; Schmitt, Stieb, et al., 2016). The BU receives sensory information from the

AOTU by extrinsic neurons innervating the TUBUT (Figure 9a). The *Cataglyphis* brain exhibits only one single BU per hemisphere which is positioned ventrolateral to the CB (Figure 7h). Its medial border is demarcated by the isthmus tract (IT), which connects the LAL with the CB (Figure 9a). The LAL lies inferior to the PED and the CL and more

FIGURE 8 Three-dimensional reconstruction of the central adjoining neuropils. The reconstructions of the neuropils were based on anti-5-HT, anti-synaps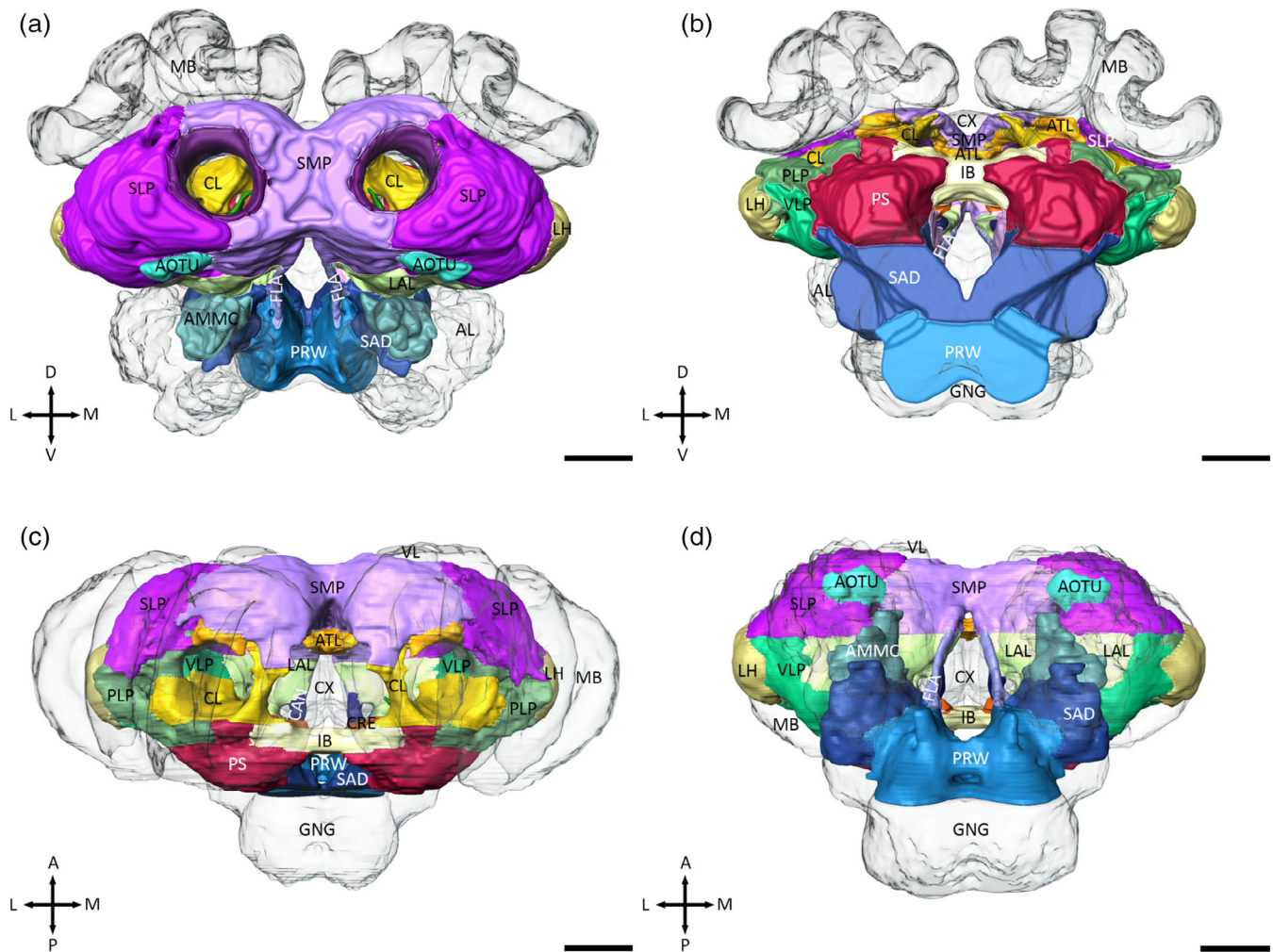in, and f-actin phalloidin staining. Antennal lobes (AL), mushroom bodies (MB), and central complex (CX) are shown in transparent. (a) Anterior view. (b) Posterior view. (c) Dorsal view. (d) Ventral view. Scale bars = 100 μm. AMMC, antennal mechanosensory and motor center; ATL, antler; CAN, cantle; CL, clamp; CRE, crepine; FLA, flange; GNG, gnathal ganglion; IB, inferior bridge; LAL, lateral accessory lobe; LH, lateral horn; LI, lip; PLP, posterolateral protocerebrum; PRW, prow; PS, posterior slope; SAD, saddle; SIP, superior intermediate protocerebrum; SLP, superior lateral protocerebrum; SMP, superior medial protocerebrum; VLP ventrolateral protocerebrum [Color figure can be viewed at wileyonlinelibrary.com]

posterior, inferior to the BU (Figure 7e–g). The inferior border is defined by thick glial processes and its medial border by the m-ALT (Figure 9a). To its lateral side, the LAL is flanked by the ventrolateral protocerebrum (VLP, Figure 7e–g). The horizontal ventrolateral protocerebrum fascicle (hVLPF) and the inferior fiber system (IFS) demarcate the boundary between these two neuropils (Figure 9a). As the anterior border between the LAL and the SMP appears to be very ambiguous, the border was set at the level of the anteriormost part of the superior fiber system (SFS). The LALs of both hemispheres are interconnected by the LAL commissure (Figure 9a).

3.7 | Superior neuropils

The superior lateral protocerebrum (SLP), the superior intermediate protocerebrum (SIP), and the superior medial protocerebrum (SMP)

form the superior neuropils (SNP). In *Cataglyphis*, the SNP are the anteriormost region of the brain (Figures 7a–f and 8a,c,d). The largest neuropils of the SNP are the SMP and the SLP. The SLP demarcates the anterolateral border of the brain and extends between the MB calyces and the AL/AOTU all across the anteriormost part of the central brain. To its medial side, the TUBUT and the PCT define the boundaries of the SMP and the SIP (Figure 9b). The superior lateral protocerebral tract (SLPT) outlines the posteroinferior boundary of the SLP to the neighboring posterolateral protocerebrum (PLP, Figures 7e,f and 9b). In contrast to dung beetles (Immonen et al., 2017), we found only one branch of the SLPT, which runs from the lateral cell body rind to the SFS (Figure 5). The SMP expands to the anteriormost part of the brain across the midline and encloses in a cup-shaped manner on both hemispheres the SIP, the VLs, and the anterolateral part of the ATL (Figures 7a–f and 9b). More posteriorly, the median bundle (MBDL) and the posteromedial part of the ATL

separate the neuropil of both hemispheres (Figures 7d and 9b). Dorsal and anteroventral, respectively, the neuropil is ensheathed by a thick layer of glial cells (Figure 7a–d). TUBUT, PCT, SFS, and AOTU demarcate the lateral borders of the SMP (Figures 7a,b and 9b). While SMP and SLP occupy relatively large areas in the brain, the SIP is much

smaller. It surrounds the VL in the anteriormost region of the brain and is encircled by the SLP, the SMP, and, more posteriorly, by the ATL and the anteriormost edge of the PLP (Figures 7a–d and 9b). As this neuropil is interspersed by many efferent neurons of the VL and the LX, it is recognizable by its less homogenous and intense
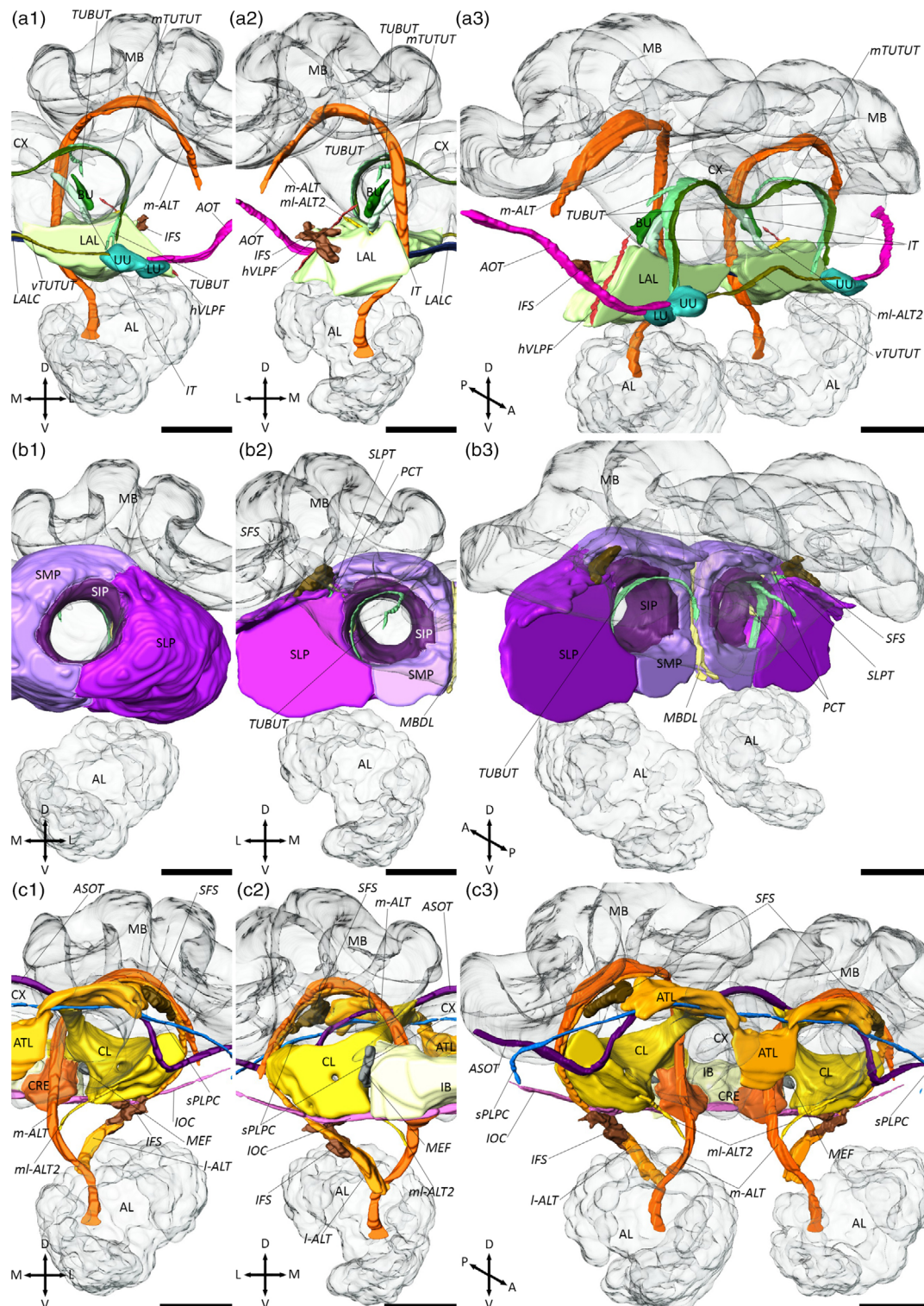

FIGURE 9 Legend on next page.

synapsin-immunoreactivity (-ir). In honey bees, this brain region has been termed ring neuropil, which is characterized by the innervation of the projection neurons from the ml-ALTs (Abel, Rybak, & Menzel, 2001; Kirschner et al., 2006).

3.8 | Inferior neuropils

The inferior neuropils (INP) occupy the medial brain region around the PED and the ML and lie posterior to the SNP and medial to the VLNP (Figures 7d–i and 8). They comprise the brain areas crepine (CRE), clamp (CL), inferior bridge (IB), and antler (ATL). The ATL and is the anteriormost neuropil of the INP. As in dung beetles (Immonen et al., 2017), the ATL extends across the midline up to the SFS and the posteromedial edge of the SLP (Figure 7d–f). The shape of the ATL is closely associated with the processes of the superior postero-lateral protocerebrum commissure (sPLPC, Figure 9c). The posterior end of the ATL is delineated by a clear glial boundary (Figure 7e,f). Its dorsal and ventral borders are enclosed by the SMP and the SIP (Figure 7d). Since the ATL and most of the neighboring neuropils are obviously contiguous, we defined the borders based on slight differences in the anti-synapsin-ir. More posteriorly in the brain are the CRE, CL, and IB located. The CL is wrapped around the posterior part of the PED and is flanked by the m-ALT and the l-ALT (Figure 9c). It extends from the CBU (dorsomedial) up to the dorsal edge of the LAL (anterior), the ventral complex (VX, posterior), and the VLNP (Figure 7f–i). The CL is separated from the neighboring SMP (superior), ATL (anterolateral), CBU (medial), m-ALT (medial), BU (medial), CRE (medial), NO (posteromedial), and the lateral MB calyx (dorsolateral, Figure 7f–i) by thick glial processes. In contrast, most boundaries to the ventral and lateral adjoining neuropils are continuous and were marked by the help of several fiber bundles: the ASOT (anterolateral), the l-ALT (lateral), the ml-ALT 2 (anteroventral), the medial equatorial fascicle (MEF, posteromedial), the IFS, and the inferior optic commissure (IOC; both ventral, Figure 9c). The CRE wraps around the ventral and lateral sides of the posterior tip of the medial lobes (Figure 7h,i). In Drosophila, this neuropil is heavily innervated by MB extrinsic neurons (Tanaka, Tanimoto, & Ito, 2008). It is surrounded by the BU and the CL (lateral), the VX (ventral), and the IB (posterior,

Figure 7h–j). On its posterior end, the boundaries of CL and CRE to the IB and the posterior slope (PS) appear rather contiguous. We therefore used the posterior tip of the MLs to set the posterior end of these neuropils. The posteriormost subregion of the INP is the IB. First identified in Musca domestica (Strausfeld, 1976), the IB is an unpaired neuropil, which is stretched across the midline. Together with the PS and the PLP, the IB forms the dorsalmost part of the posterior cerebrum in Cataglyphis (Figure 7j). The IB is laterally separated from the PS by the MEF. The ventral boundary of the IB and the VX, in turn, is defined by the IOC, respectively (Figures 7j and 9c).

3.9 | Lateral horn

The LH is one of the most prominent neuropils of the CANP. It receives direct sensory input from all ALTs (Figure 6a) and demarcates the lateral border of the cerebrum (Figures 7d–h and 8). The boundaries of the LH were determined based on the innervation by projection neurons traced along the ALTs. In addition, the LH can be distinguished by its brighter synapsin-ir in comparison to its adjacent neuropils. Medial to the LH lie the SLP, the PLP, and more ventral, the VLP (Figures 7d–h and 10a).

3.10 | Ventrolateral neuropils

The ventrolateral neuropils (VLNP) consist of the ventrolateral protocerebrum (VLP) and the posterolateral protocerebrum (PLP). They are located posterior to the SNP and ventrolateral to the INP (Figures 7e–j and 8b–d). The VLNP covers a large area in the Cataglyphis brain, expanding from the AL up to the OL and from the anteriormost part of the SFS up to the posteriormost regions of the IFS and lateral equatorial fascicle (LEF, Figures 7e–j and 10a). While the boundaries on the superior and inferior sides are obviously separated by extensive glial sheaths, the medial/lateral, and anterior/posterior junctions to neighboring neuropils are very often contiguous (Figure 7e–j). In Drosophila, the VLP is divided into an anterior (anterior ventrolateral protocerebrum [AVLP]) and posterior part (posterior

FIGURE 9 Three-dimensional reconstruction of individual central adjoining neuropils and associated fiber bundles. Antennal lobes (AL), mushroom bodies (MB), and central complex (CX) are shown in transparent. All neuropils are shown from anterior (1), posterior (2), and anterolateral (a3, c3), or posterolateral (b3). (a) Lateral complex (LX), anterior optic tubercle (AOTU), and associated fiber bundles. The LX can further be divided into the bulb (BU) and lateral accessory lobe (LAL). The AOTU consist of an upper (UU) and lower unit (LU). For the demarcation of the neuropils, the horizontal ventrolateral protocerebrum fascicle (hVLPF), the isthmus tract (IT), the inferior fiber system (IFS), the lateral accessory lobe commissure (LALC), the medial antennal lobe tract (m-ALT), the medial tubercle-tubercle tract (mTUTUT), the mediolateral antennal lobe tract 2 (ml-ALT 2), the tubercle-bulb tract (TUBUT), and the ventral tubercle-tubercle tract (vTUTUT) were used. (b) Superior neuropils and associated fiber bundles. The superior neuropils consist of the superior intermediate protocerebrum (SIP), the superior lateral protocerebrum (SLP), and the superior medial protocerebrum (SMP). The median bundle (MBDL), the protocerebral-calycal tract (PCT), the superior lateral protocerebrum tract (SLPT), and the TUBUT were used as landmarks to define the boundaries of the superior neuropils. (c) Inferior neuropils and associated fiber bundles. The inferior neuropils comprise the antler (ATL), the clamp (CL), the crepine (CRE), and the inferior bridge (IB). Important fiber bundles for the demarcation of these neuropils are the inferior fiber system (IFS), the inferior optic commissure (IOC), lateral antennal lobe tract (l-ALT), the medial equatorial fascicle (MEF), the ml-ALT 2, the superior fiber system (SFS), and the superior posterolateral protocerebrum (sPLPC). Scale bars = 100 μm [Color figure can be viewed at wileyonlinelibrary.com]
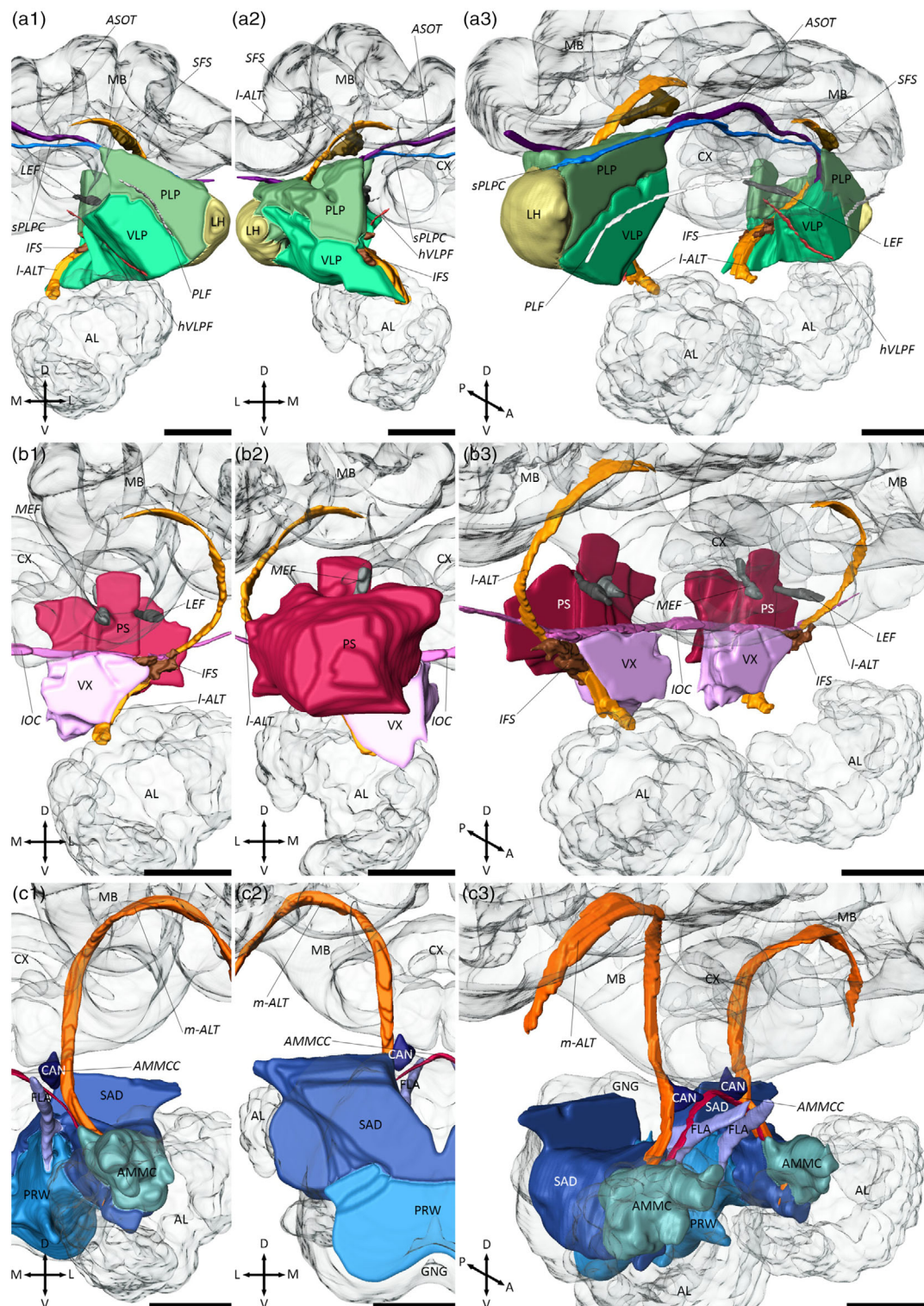
FIGURE 10 Three-dimensional reconstruction of individual central adjoining neuropil groups and associated fiber bundles (continuing from Figure 9). All neuropil groups are shown in anterior (1), posterior (2), and anterolateral view (3). (a) Ventrolateral neuropils (VLNP), lateral horn (LH), and associated fiber bundles. The posterolateral protocerebrum and the ventrolateral protocerebrum form the VLNP. The anterior superior optic tract (ASOT), the inferior fiber system (IFS), the lateral antennal lobe tract (l-ALT), the lateral equatorial fascicle (LEF), the superior posterolateral protocerebrum commissure (sPLPC), and the horizontal ventrolateral protocerebrum fascicle (hVLPF) are used to define the boundaries of the neuropils. (b) Ventromedial neuropils (VMNPs) and associated fiber bundles. The posterior slope (PS) and the ventral complex are the VMNP in the *Cataglyphis* brain. To demarcate the borders of the VMNP, the l-ALT, the IFS, the inferior optic commissure (IOC), the LEF, and the medial equatorial fascicle (MEF) were used. (c) Periesophageal neuropils (PENP) and associated fiber bundles. The PENP consist of the antennal mechanosensory and motor center (AMMC), the cantle (CAN), the flange (FLA), the prow (PRW), and the saddle (SAD). Important fiber bundles as landmarks for the demarcation of the PENP are the medial antennal lobe tract (m-ALT) and the antennal mechanosensory and motor center commissure (AMMCC). Scale bars = 100 μm [Color figure can be viewed at wileyonlinelibrary.com]

ventrolateral protocerebrum [PVLP]) based on a more glomerular structure of the PVLP in comparison with the AVLP (Ito et al., 2014; Otsuna & Ito, 2006). However, no structural differences could be recognized in this region in *Cataglyphis*, and thus, the neuropil was not further divided into subregions. Unlike in dung beetles (Immonen et al., 2017), the VLP is not characterized by an enriched serotonergic innervation. We therefore defined the borders based on several fiber bundles: the ASOT (superior), the posterior lateral fascicle (PLF, superolateral), the l-ALT (superomedial), the hVLPF, and the IFS (both medial, Figure 10a). The PLP is demarcated by the sPLPC (superior), the PLF (inferomedial) the ASOT (anteromedial), the l-ALT (medial), and the LEF (posteromedial, Figure 10a). Lateral to the VLNPs is the LH attached (Figure 7e–h).

3.11 | Ventromedial neuropils

Ventral complex (VX) and posterior slope (PS) form the ventromedial neuropils (VMNP) of the *Cataglyphis* brain. They are located posterior to the INP and flank the esophagus on both hemispheres of the brain (Figures 7h–l and 8b,c). Because of a lack of unambiguous landmarks, VX and PS were not further divided into subcompartments (namely vest, gorget, and epaulette; superior and inferior PS). The IFS is the most important landmark to localize the VX in the brain of *Cataglyphis*. It defines the anterior and posterior end of the neuropil and demarcates, together with the l-ALT, the lateral borders to the VLP (Figure 10b). In addition, the IOC serves as an apparent dorsal boundary to the neighboring CRE, BU, CL, and more posterior, IB and PS (Figures 7h–j and 10b). In contrast, the ventral boundaries to the prow (PRW) and the saddle (SAD) are rather contiguous but due to a more intense synapsin-ir of the PRW still is clearly recognizable (Figure 7h–j). The PS starts at the level of the IB and is situated at its anteriormost part between IB and PLP, whereas LEF and MEF form the lateral and medial borders (Figures 7j and 10b). More posterior, the PS expands from the esophagus to the lateral edge of the cerebrum. The SAD and the GNG are localized ventral to the PS (Figure 7k,l).

3.12 | Periesophageal neuropils

The periesophageal neuropils (PENP) in the *Cataglyphis* brain comprises the regions of the cantle (CAN), flange (FLA), prow (PRW), and the saddle (SAD), which houses the antennal mechanosensory and motor center (AMMC). These neuropils form the ventralmost region of the brain around the esophagus between the AL and the GNG (Figures 7e–k and 8). The AMMC is the most prominent and probably best studied neuropil of the PENP. It receives primary mechanosensory input from the antennae, providing information about position and movement of the antennae (Ai, Nishino, & Itoh, 2007; Ehmer & Gronenberg, 1997; Homberg, Christensen, & Hildebrand, 1989; Kamikouchi et al., 2009), and gustatory input in a variety of insects (Farris, 2008; Jørgensen, Kvello, Almaas, &
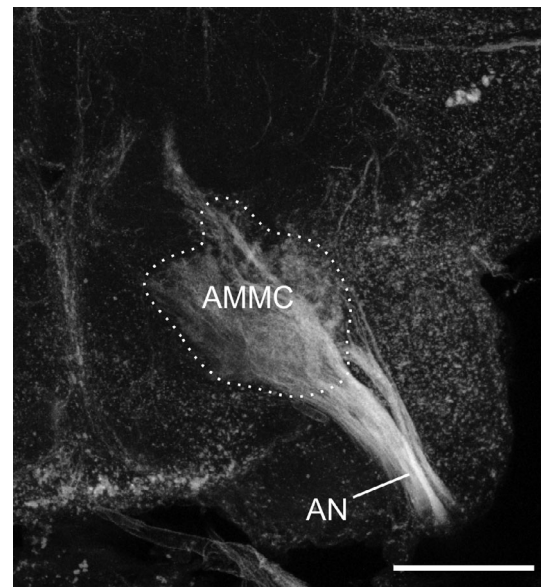

FIGURE 11 Projection of the antennal nerve (AN) into the antennal mechanosensory and motor center (AMMC). Microruby was used for the anterograde staining. Z-projection from a stack of 21 images with 5 μm step size. Scale bar = 100 μm

Mustaparta, 2006; Miyazaki & Ito, 2010). To accurately define the borders of the AMMC, in particular to the SAD, we performed AN backfills (Figure 11). In *Cataglyphis*, the AMMC is adjacent to glomeruli of the AL and more posteriorly it merges smoothly into the SAD (Figure 7c–g). The SAD is a relatively large neuropil and is situated between the LAL and the AL (Figure 7g). More posteriorly, it lies beneath the VX, the VLP and superolateral to the PRW (Figure 7h–j). In its posteriormost region, the neuropil is connected across the midline and its boundaries to the adjacent PS (superior) and the GNG (posterolateral) appear rather contiguous (Figures 7k and 10c). In contrast to the SAD, the CAN is a very small and paired neuropil with clear borders (Figures 7g,h and 10c). In *Cataglyphis*, it fills out a triangular-shaped area in between of the ML (superior), the m-ALT (lateral), and the esophagus (medial, Figure 7g,h and 10c). The ventral boundary of the CAN is defined by the AMMC commissure which interconnects the AMMCs of both hemispheres (Figure 10c). Neighboring neuropils are the LAL (lateral), the VX (inferolateral), the SAD (inferolateral), and the FLA (ventral, Figure 7g,h). Unlike in *Drosophila* (Ito et al., 2014), the FLA is heavily surrounded by thick glial processes in *Cataglyphis*. Due to its bar-shaped structure and unambiguous borders, it is easily distinguishable from the surrounding neuropils such as the LAL and the SAD (both lateral). It emerges at the root of the MBDL, where it extends lateral from the esophagus and extends up to the anterior tip of the PRW (Figures 7e–h, 8a,d, and 10c). The last and most ventral structure of the PENP is the PRW. The structure of this neuropil appears brighter in the anti-synapsin staining than in the remaining adjoining neuropils. Its neighbors are the VX (superior), the FLA (anterior), the SAD (superolateral), and the GNG (posterolateral, Figures 7h–l and 8a,d).

3.13 | Visual fibers

To generate an overview of all visual tracts and commissures and their target neuropils, we used neuronal tracer injections into the ME and LO and projected them into the map of synapsin-rich neuropils in the *Cataglyphis* brain. One of the most prominent visual fiber bundles in Hymenoptera is the ASOT to the lateral and medial calyces of the MBs. The ASOT forms side branches into the ipsilateral and contralateral CO of the MB calyces (Figures 12a–c,h, 13, and 14b). The ASOT predominantly comprises OL neurons of the ME but also houses a small number of neurons originating from the LO (Figure 12a–c). In contrast to our findings, in honey bees the LO projections run in a separate tract (LO tract) before they join the ASOT (Ehmer & Gronenberg, 2002; Mobbs, 1984). The ASOT can be found anterior in the brain and exhibits a characteristic course through the brain with a sharp bend lateral to the PED, just before it passes the VLs superiorly and crosses the midline dorsal to the CX (Figures 12a–c,h, 13, and 14b). In *Cataglyphis*, the ASOT is not the only visual fiber tract with projections into the MBs. Our tracer injections revealed a second fiber tract of unknown identity that runs anterior to the ASOT and dorsal to the SLP, which we termed optical calycal tract (OCT). The OCT interconnects the ME and LO with the ipsilateral MB CO but, in contrast to the ASOT, does not project into the contralateral brain hemisphere (Figures 12a–c, 13, and 14a).

In addition to these two fiber bundles, we found further tracts and commissures that project into different regions of the central brain or interconnect the OLs. We identified a very thin and serpentine shaped commissure—the serpentine optic commissure (SOC) (Figure 12h), which has also been described in the honey bee (Hertel & Maronde, 1987; Hertel, Schäfer, & Maronde, 1987). The general shape of this extremely thin commissure has strong similarities to the ASOT. In contrast to the ASOT, the SOC is situated slightly more posteriorly in the brain and consists of fibers from only a few neurons, which project from the ME and LO to their contralateral counterparts without any further arborizations into other neuropils (Figures 12a–c,h, 13, and 14b). The SOC neurons enter the central brain either ventrally to the ASOT (anterior in the brain) or more posteriorly, together with the neurons of the posterior optic commissure (POC) (Figure 12h). All SOC neurons merge at the inferolateral edge of the CL before they together pass the PE through the CL and cross the midline anterior to the CBU slightly ventral to the ASOT (Figures 12h and 14b).

Another very prominent tract in all insect brains investigated so far is the AOT (Figures 12a–c,g, 13, and 14a). In *Cataglyphis*, the AOT is situated inferolaterally of the SLP and anteriorly to the LH. Among others, it transfers information from the sky polarization pattern from the OLs to the AOTU (el Jundi et al., 2011; Pfeiffer & Kinoshita, 2012; Zeller et al., 2015). In *Cataglyphis*, the AOT is accompanied by additional neurons that pass the AOTU and run into the VX (Figures 12g, 13, and 14a). Both subunits of the AOTU as well as the VX are supplied by projection neurons of the ME and the LO (Figure 12a–c,g).

In addition, we found two further commissures, the POC and the IOC. Both commissures have previously been reported in honey bees (DeVoe, Kaiser, Ohm, & Stone, 1982; Hertel et al., 1987; Hertel & Maronde, 1987; Mobbs, 1984) and in the ant *Camponotus rufipes* (Yilmaz et al., 2016). In *Cataglyphis*, POC and IOC contain projection neurons of the ME and the LO (Figure 12d–f). The POC is the thickest visual fiber bundle in the *Cataglyphis* brain and easily recognizable in the immunostaining, even without any further anterograde tracing. After the commissure emerges from the OLs, it enters the cerebrum just ventral to the posterior part of the LCA and exhibits many ramifications into the VLNPs (Figures 12d–f, 13, and 14c). From there, the POC runs inferior to the calyces and superior to the PLP before it bifurcates into two relatively thick branches. One neuronal bundle exits the commissure ventrally and innervates the VMNPs (Figures 12d–f, 13, and 14c). The remaining neurons of the POC continue along a more or less straight line in between the CA and the PS before they cross the midline above the IB (Figure 12d–f). Close to the midline, some of these neurons bifurcate into the ocellar tracts (Figure 12i). The IOC lies inferior to the POC (Figures 12d–f, 13, and 14c). In *Cataglyphis*, this commissure separates PLP (superior) and VLP (inferior) as well as CL/CRE (superior) and VX (inferior) before it crosses the midline of the brain. Lateral to the l-ALT, many neurons of the IOC leave the commissure ventrally and innervate the VLNPs. In addition, the IOC gives rise to medial arborizations into the VX (Figures 12d–f, 13, and 14c).

4 | DISCUSSION

In this study, we examined the brain of the worker caste in the thermophilic ant *Cataglyphis nodus*, a favorable experimental model for the study of long-distance navigation. These ants are perfectly adapted to harsh environments with very high ground temperatures and scattered food resources, which they predominantly find during largely visually guided foraging trips. Overall, we reconstructed 25 paired and 8 unpaired synapse-rich neuropils, defined 30 fiber tracts, among them 6 fiber tracts that provide new insights into the complexity of the visual system of the ants. A comparably detailed description of an insect brain that also includes the brain regions of the CANP currently exists only for the fruit fly *Drosophila melanogaster* (Ito et al., 2014; Pereanu et al., 2010), the monarch butterfly *Danaus plexippus* (Heinze & Reppert, 2012), the ant *Cardiocondyla obscurior* (Bressan et al., 2015), the dung beetle *Scarabaeus lamarcki* (Immonen et al., 2017) and the desert locust *Schistocerca gregaria* (von Hadeln et al., 2018). The orientation, structure, and overall layout of the *Cataglyphis* brain show large similarities with the honey bee brain (Brandt et al., 2005; Ribi, Senden, Sakellariou, Limaye, & Zhang, 2008) and appears similar across ant species, at least for the major neuropils like AL, MB, OL, and other distinct and easy recognizable neuropils. However, marked differences in relative volumes are present, for example like small optic neuropils in highly olfactory ants such as *Atta* or *Pheidole* (Groh, Kelber, Grübel, & Rössler, 2014; Ilieş, Muscedere, & Traniello, 2015), less visual *Camponotus* species (Yilmaz et al., 2016),
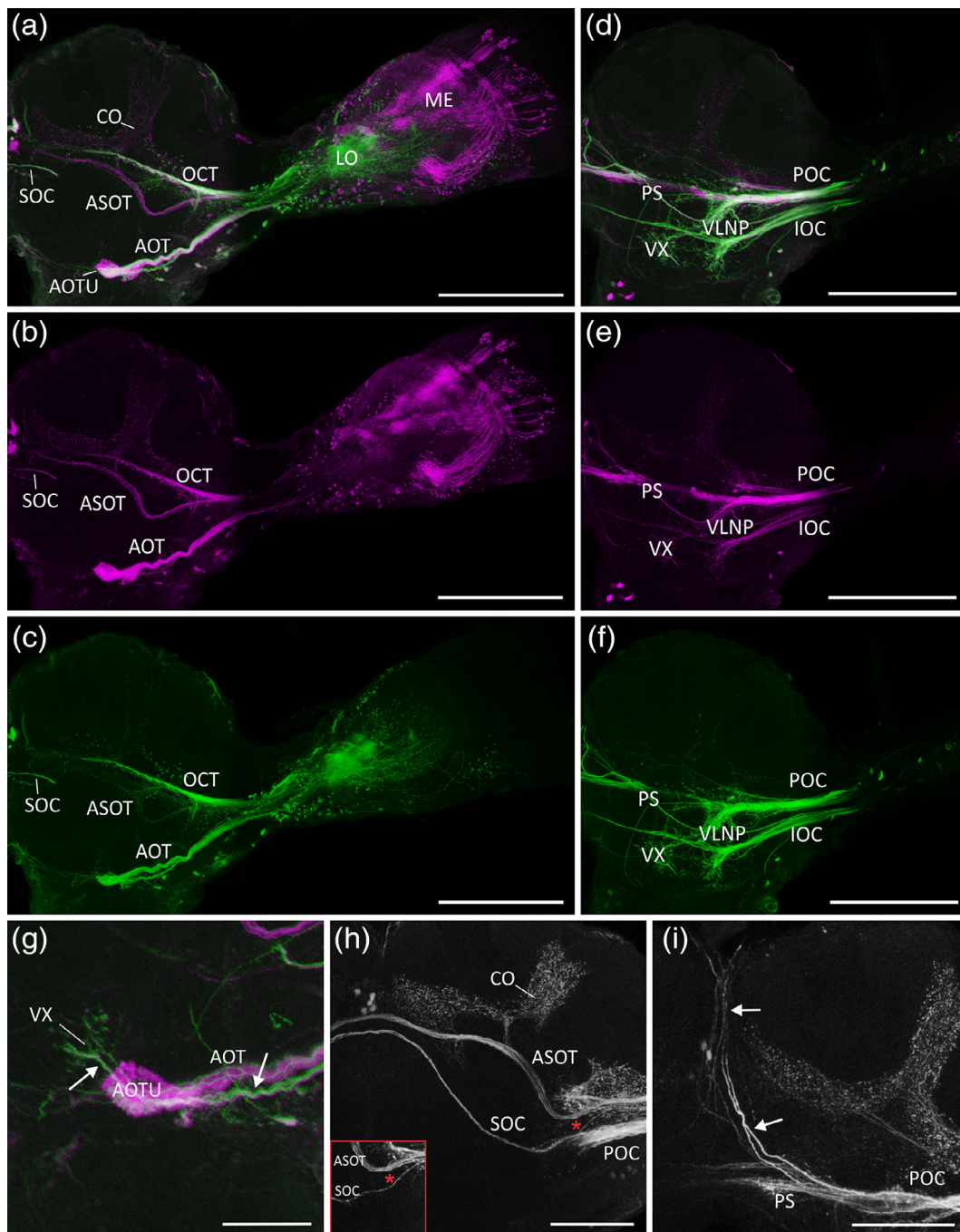
FIGURE 12   Visual projections from the optic lobes into the central brain. Anterograde staining obtained from dye injections into the medulla (ME; microruby in magenta or gray) and lobula (LO; Alexa 488 dextran in green). (a–c) Visual fiber bundles of the ME (a, b) and the LO (a, c) located in the anterior brain. Anterior optic tract (AOT), anterior superior optic tract (ASOT), optical calycal tract (OCT), and superior optic commissure (SOC) comprise all projection neurons from ME and LO. The ASOT and the OCT project into the collar (CO) of the mushroom body and the AOT into the anterior optic tubercle (AOTU). Z-projection from a stack of 20 images with 5 μm step size. Scale bars = 200 μm. (d–f) Visual fiber bundles of the ME (d, e) and LO (d, f) located in the posterior brain. The inferior (IOC) and posterior (POC) optic commissure comprise both neurons from ME and LO and project into the ventrolateral neuropils (VLNP) and the ventral complex (VX). In addition, the POC exhibits projections into the posterior slope (PS). Z-projection from a stack of 14 images with 5 μm step size. Scale bars = 200 μm. (g) The AOT is accompanied by some neurons, which run into deeper layers of the brain and innervate there the ventral complex (neurons are indicated by white arrows). Z-projection from a stack of 24 images with 5 μm step size. Scale bar = 50 μm. (h) The SOC exhibits no projections into the protocerebrum. The SOC neurons originate either from the POC or ventral to the ASOT (indicated by the asterisk, inset). Z-projection from a stack of 13 images or eight images (inset) with 5 μm step size. Scale bar = 100 μm. (i) The POC is accompanied by some neurons with projections to the ocellar tracts (indicated by white arrows). Z-projection from a stack of 10 images with 5 μm step size. Scale bar = 100 μm [Color figure can be viewed at wileyonlinelibrary.com]
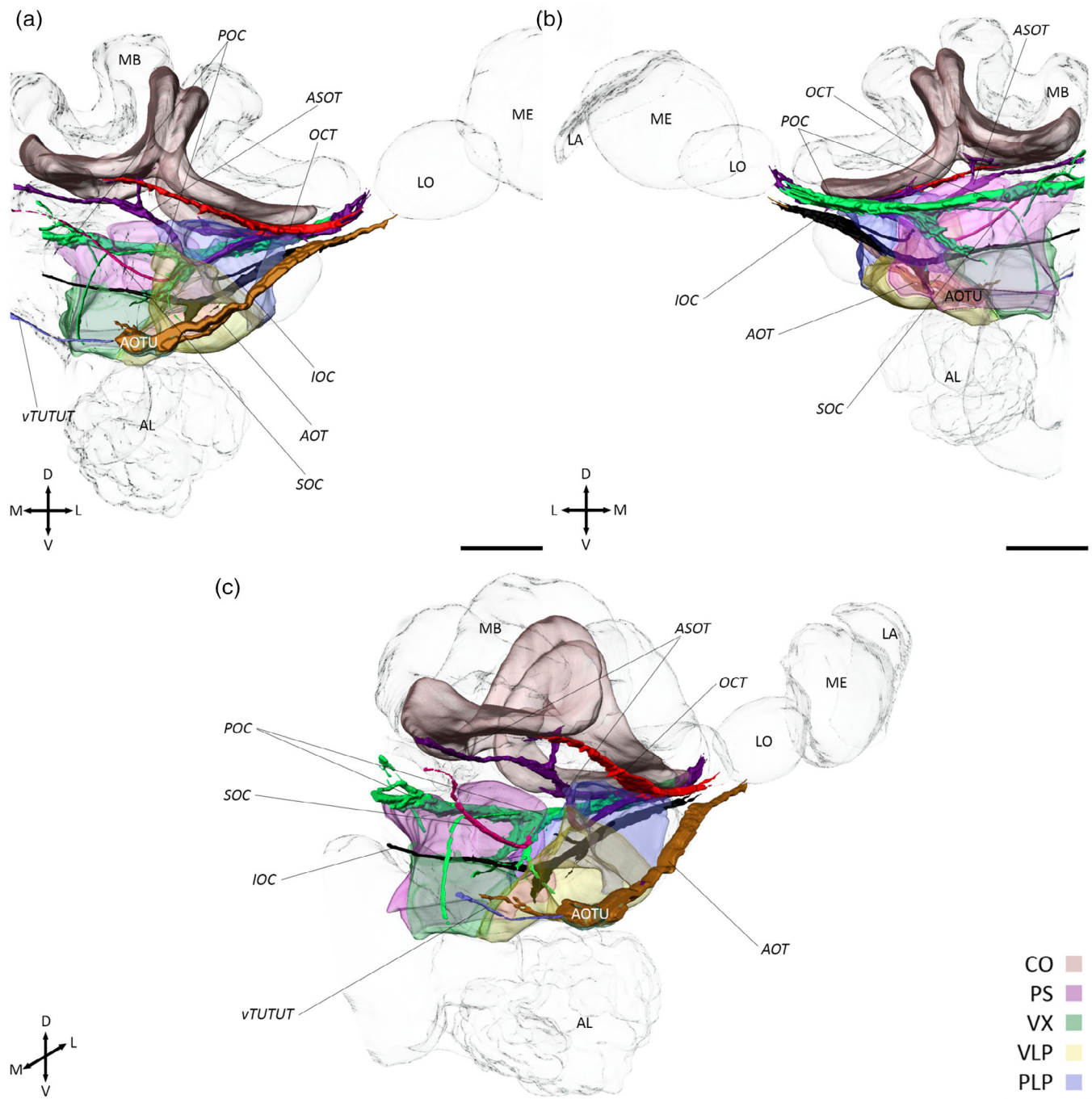
FIGURE 13 Surface reconstructions of the visual fiber bundles and their target neuropils. The surface reconstructions of the fiber bundles are based on anterograde staining and in case of the neuropils on anti-synapsin labeling. Two major optic tracts (AOT, Anterior optic tract; OCT, Optical calycal tract) and four optic commissures (ASOT, anterior superior optic tract; IOC, inferior optic commissure; POC, posterior optic commissure; SOC, serpentine optic commissure) were found. The OCT projects into the collar (CO) of the ipsilateral mushroom body and the AOT into the anterior optic tubercle (AOTU). The AOTUs are interconnected by the ventral tubercle-tubercle tract (vTUTUT). In addition, the AOT is accompanied by some neurons which project into the ventral complex (VX). The SOC is the only commissure without any ramifications into the cerebrum. The ASOT exhibits arborizations into the CO, the IOC into the posterolateral protocerebrum (PLP), the ventrolateral protocerebrum (VLP) and the ventral complex (VX), and the POC into the PLP, the VLP, the VX, and the posterior slope (PS). (a) Anterior view. (b) Posterior view. (c) Anteromedial oblique view. Scale bars = 100 μm. LA, lamina; LO, lobula; ME, medulla [Color figure can be viewed at wileyonlinelibrary.com]

or *Cardiocondyla obscurior* (Bressan et al., 2015). A most striking difference is the orientation of the brain. While the central brains of other insects, including dipterans, lepidopterans, and coleopterans (el Jundi et al., 2009; Heinze & Reppert, 2012; Immonen et al., 2017; Ito et al., 2014) tilt during the metamorphic development by 90° (Huetteroth, el Jundi, el Jundi, & Schachtner, 2010), the brains of
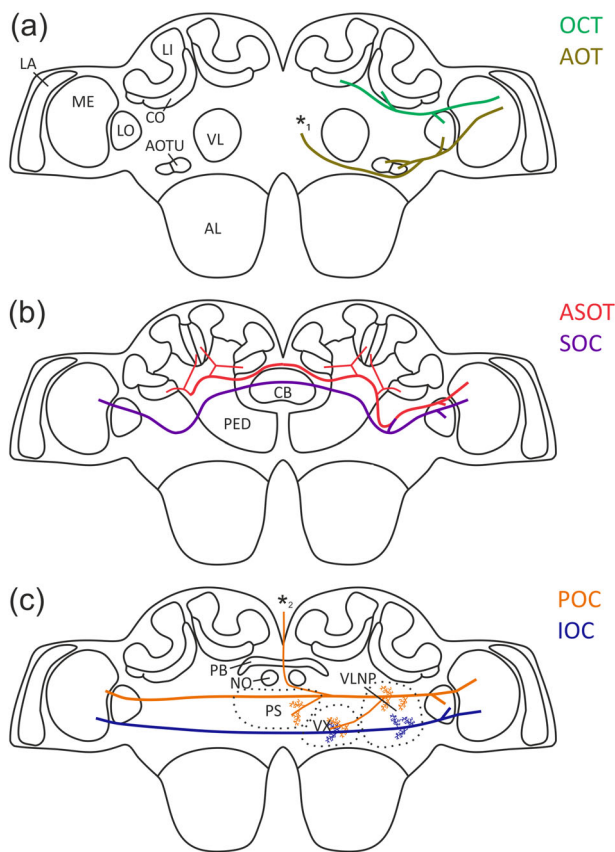
FIGURE 14 Schematic drawing of the visual fiber bundles of the *Cataglyphis nodus* brain. The overview of the optical tracts and commissures based on anterograde staining received from dye injections into the medulla (ME; microruby) and lobula (LO; Alexa 488 dextran). (a) The optical calycal tract (OCT) and the anterior optic tract (AOT) are situated in the anterior part of the brain. The OCT projects into the ipsilateral collars (CO) of the mushroom bodies (MB) and the AOT into the ipsilateral anterior optic tubercle (AOTU). Both tracts receive input from the medulla (ME) and lobula (LO). The AOT is additionally accompanied by some neurons, which run into deeper layers of the brain, innervating the ventral complex (VX, indicated by asterisk 1). (b) The anterior superior optic tract (ASOT) and the serpentine optic commissure (SOC) are situated more posteriorly than AOT and OCT but still relatively far anterior in the brain. The SOC connects the ME and LO with their contralateral counterparts. The ASOT has ramifications into the ipsi- and contralateral COs. (c) The posterior optic commissure (POC) and the inferior optic commissure (IOC) are situated in the posterior part of the brain. Both commissures connect the MEs and LOs between the hemispheres. The POC has ramifications into the dorsal region of the ventrolateral neuropils (VLNP), the ventral complex (VX), and the posterior slope (PS). In addition, some neurons, which accompany the POC, connect the optic lobes with the ocelli (indicated by asterisk 2); the IOC innervates the ventrolateral part of the VLNP and the VX. AL, antennal lobe; CB, central body; LA, lamina; LI, lip; NO, noduli; PB, protocerebral bridge; PED, pedunculus [Color figure can be viewed at wileyonlinelibrary.com]

hymenopterans do not undergo such a modification. Thus, the central brain of, for example, ants, honey bees, wasps, and also hemimetabolous insects like locusts (Brandt et al., 2005; Groothuis et al., 2019; Kurylas, Rohlfing, Krofczik, Jenett, & Homberg, 2008) are oriented

perpendicular compared to, for example, the fly brain. It was therefore not trivial to compare and identify similar brain regions in the ant brain using those described in the fly brain. Nevertheless, our description of the neuropils, tracts, fibers and commissures can serve as a reliable base for the brains of other ant species, bees, and wasps.

4.1 | Mushroom bodies and visual input

Cataglyphis ants, like honey bees, possess very prominent and complex MBs (Figures 1 and 3): each MB consists of a medial and a lateral calyx, and each of these calyces, in turn, can further be subdivided into a CO and LI region. This subdivision most likely is a consequence of the high importance of visual memory, in addition to olfactory memory (Gronenberg, 1999; Hertel & Maronde, 1987; Mobbs, 1984; Paulk & Gronenberg, 2008; Yilmaz et al., 2016). Therefore, the MBs in *Cataglyphis* represent a truly multimodal integration center (Figures 6a,b and 12a–c,h) (Gronenberg, 1999, 2001). The expansion of visual innervation of the MB calyx in species along the hymenopteran lineage first occurs in species with parasitoid lifestyles as well as in all social species, and, therefore, was interpreted as a trait that co-occurred with advanced spatial orientation (Farris & Schulmeister, 2010). The importance of the MBs for learning and memory has been extensively demonstrated in honey bees (Erber, Masuhr, & Menzel, 1980; Menzel, 1999, 2001; Szyszka, Galkin, & Menzel, 2008) and can be assumed to serve a similar function in *Cataglyphis*. Although the exact number of KCs of the MBs in *Cataglyphis* is not known, it can be assumed to be very high compared to many other insects. For example, the MB of the ant *Camponotus rufipes* houses around 130,000 KC (Ehmer & Gronenberg, 2004). As the visual MB COs in *Cataglyphis* have large volumes and contain an estimated total number of ~400,000 microglomeruli (Grob et al., 2017; Grob et al., 2019), compared to ~160,000 in *Camponotus rufipes* (C. Groh, personal communication), we assume that the total number of associated KCs may be even higher in *Cataglyphis*. Therefore, KC numbers in *Cataglyphis* MBs are likely as high as in *Camponotus* with a decent number of KCs associated with the large CO region (Figure 3) (Gronenberg & Hölldobler, 1999). However, as the relationship between KC numbers and microglomeruli may differ between ant species, this requires further investigations. Comparison with honey bees suggest that the KC numbers are of the same order (340,000 KCs) (Rössler & Groh, 2012; Strausfeld, 2002; Witthöft, 1967) and much higher than in *Drosophila* MBs (2,500 KC) (Fahrbach, 2006). The discrepancy between *Drosophila* and aculeate hymenopteran MBs most likely concerns differences in navigational abilities and the socio-ecological context of social Hymenoptera. As outlined above, the correlation between advanced spatial orientation with the visual input and expansion of the MBs in higher Hymenoptera was proposed in several studies (Farris, 2013, 2015; Farris & Schulmeister, 2010).

Our study shows that several fibers and commissures transfer visual input into the MBs of *Cataglyphis nodus*, which likely causes the relatively large CO region containing a high number of input synaptic complexes (microglomeruli) (Grob et al., 2017; Stieb et al., 2012). The

large MBs, in general, and the substantial amount of visual input into the CO are in line with the excellent abilities of *Cataglyphis nodus* and other *Cataglyphis* species to form visual memories for landmarks and/or panoramic sceneries as shown or highlighted more recently (Fleischmann, Christian, Müller, Rössler, & Wehner, 2016; Fleischmann et al., 2018; for reviews, see Rössler, 2019; Zeil & Fleischmann, 2019). *Cataglyphis* foragers have to learn the visual features of their nest surroundings in order to find their way to their nest entrance when homing back from foraging trips (Cruse & Wehner, 2011; Wehner & Menzel, 1969; Wehner & Räber, 1979). Several studies suggest that the latter is achieved by taking snapshots of the panorama during specific learning walks when the ants leave their nest for the first time (Fleischmann, Grob, Wehner, & Rössler, 2017; Müller & Wehner, 1988). This visual information, most likely, is stored in the vast number of associative visual microcircuits that involve many thousands of KCs. It appears counterintuitive, however, that the basal ring, a substructure known from honey bees, is not a distinct structure in *Cataglyphis* MBs, especially as the basal ring is known as a multimodal sensory input region integrating visual and olfactory stimuli (Gronenberg, 1999, 2001). However, also in other ant species, the basal ring is largely reduced, possibly absent, or indistinguishable from the CO (Ehmer & Gronenberg, 2004; Gronenberg, 1999). The reasons for this remain unclear.

4.2 | Antennal lobes and dual olfactory pathway

Recent studies showed that the ALs of *C. nodus* workers contain about 226 glomeruli, which is in a similar range to other *Cataglyphis* species such as *C. fortis* (~198) and *C. bicolor* (~249) (Stieb et al., 2011). However, this number is substantially smaller compared to high glomeruli numbers in other ant species, such as *Camponotus floridanus* (~434) (Zube et al., 2008), *Camponotus japonicus* (~438) (Nishikawa et al., 2008), the wood ant *Formica rufibarbis* (~373) (Stieb et al., 2011), or the high numbers in leaf cutting ants, for example *Atta vollenweideri* (Kelber, Rössler, Roces, & Kleineidam, 2009). The reduced number of glomeruli might reflect the different ecology of *Cataglyphis* ants that, compared to all other species mentioned above, primarily rely on visual information instead of pheromonal cues during foraging (Ruano et al., 2000; reviewed by: Wehner, 2003). On the other hand, studies have shown that *Cataglyphis* do use olfactory cues during cross wind orientation while searching for food (Buehlmann et al., 2014; Steck, Hansson, & Knaden, 2011). However, both the role of pheromones and food odors may be minor compared to ants with reduced visual capabilities. In any case, compared to non-social insects, for example, *Drosophila* (~40) (Laissue et al., 1999; Stocker, Lienhard, Borst, & Fischbach, 1990; Wong, Wang, & Axel, 2002), lepidopterans (~ 50–70) (Masante-Roca, Gadenne, & Anton, 2005; Montgomery & Ott, 2015; Varela et al., 2009), and dung beetles (~ 85) (Immonen et al., 2017), the number of olfactory glomeruli in *Cataglyphis* still are comparatively high most likely due to social interactions and communication inside the nest using cuticular hydrocarbon cues (Hölldobler & Wilson, 1990).

We also found that *Cataglyphis* possess a dual olfactory pathway, similar to the previously described feature in various other higher hymenopterans (Brill, Meyer, & Rössler, 2015; Couto, Lapeyre, Thiéry, & Sandoz, 2016; Kirschner et al., 2006; Rössler & Zube, 2011; Zube et al., 2008). Like in other Hymenoptera, projection neurons of different subpopulations of glomeruli and projection neurons form the major tracts m-ALT, l-ALT, and the three thinner ml-ALTs in *Cataglyphis* (Figure 6a). This feature appears more complex compared to most other insect species, with a smaller number of AL output tracts (reviewed by Galizia & Rössler, 2010). Functional studies suggest that both parallel processing and coincidence coding are employed within this system leading to enhanced coding capabilities for these insects with highly complex olfactory environments and behaviors (Brill et al., 2013; Brill et al., 2015; Carcaud, Giurfa, & Sandoz, 2015; Müller, Abel, Brandt, Zöckler, & Menzel, 2002; Rössler & Brill, 2013).

4.3 | Optic lobes

The OLs in the *Cataglyphis* brain are relatively large in comparison to other ant species (Figure 1) (Gronenberg & Hölldobler, 1999). Enlarged OLs are otherwise typically present in winged, reproductive castes or visually hunting ants, which underpins the high relevance of visual stimuli for visually based navigation in *Cataglyphis* workers. The OLs of *Cataglyphis* show the typical structure with LA, ME, and LO (Figure 2) (Brandt et al., 2005; Gronenberg, 2008; Gronenberg & Hölldobler, 1999). In contrast to Diptera, Coleoptera, Lepidoptera, or Trichoptera, *Cataglyphis* possess one coherent LO instead of an LO complex that consists of two distinct areas: LO and LO plate. In many insects, the LO plate is a center for motion vision that encodes optic-flow information (Hausen, 1976; Hausen, 1984; Joesch, Plett, Borst, & Reiff, 2008). However, studies in *Cataglyphis bicolor* have shown that the ants perceive optic-flow information and use it for distance estimations (Pfeffer & Wittlinger, 2016). This raises the question how optic-flow information is processed in the ant brain, more explicitly whether the LO can further be subdivided into different functional subregions, similar to what has been shown for the praying mantis and the locust (Kurylas et al., 2008; Rosner, von Hadeln, Salden, & Homberg, 2017) or in other hymenopteran species (Paulk & Gronenberg, 2008; Strausfeld, 2012).

4.4 | Central complex, anterior optic tubercle, and lateral complex

In *Cataglyphis*, the AOTU comprises an upper and a lower subunit which seems to be highly conserved in all insects studied so far (el Jundi et al., 2010; Heinze & Reppert, 2012; Immonen et al., 2017; Montgomery, Merrill, & Ott, 2016; Mota et al., 2011; Strausfeld & Okamura, 2007; von Hadeln et al., 2018). In all insects, sky-compass neurons project into the lower subunit of the AOTU whereas the upper division is associated with chromatic, unpolarized-light vision (Mota et al., 2011; Mota et al., 2013; Pfeiffer & Kinoshita, 2012; Zeller

et al., 2015). In *Cataglyphis*, the AOTUs on both sides are connected via the TUBUT (Figure 9c) and transmit sky-compass information to the BU, similar to what has been shown in other insects studied so far (el Jundi & Homberg, 2010; Heinze & Reppert, 2012; Pfeiffer et al., 2005).

While the boundaries of the LAL of the LX, a region that mediates motor output to the ventral nerve cord (Namiki & Kanzaki, 2016; Turner-Evans & Jayaraman, 2016), are more difficult to align, the BUs are easily recognizable in *Cataglyphis* due to the existence of large microglomerular synaptic structures (Figures 3g and 4d). These microglomeruli gate sky compass and other visual information before entering the lower unit of the CB via tangential neurons (Heinze & Reppert, 2012; Pfeiffer & Homberg, 2007; Seelig & Jayaraman, 2013). Interestingly, precocious stimulation of the ants with UV-light was shown to cause an increase in the number of microglomeruli in the BUs of *Cataglyphis fortis* indicating a substantial level of structural plasticity in these synaptic circuits (Schmitt, Stieb, et al., 2016). *Cataglyphis* has only one BU per hemisphere, like *Drosophila* (Seelig & Jayaraman, 2013), monarch butterflies (Heinze et al., 2013), and dung beetles (el Jundi et al., 2018) while locusts and honey bees possess two distinct BUs or groups of microglomerular complexes (el Jundi et al., 2014; Heinze & Homberg, 2008; Mota et al., 2016; Träger, Wagner, Bausenwein, & Homberg, 2008; von Hadeln et al., 2018). The reason for these differences are currently not known.

We could also define the IT in *Cataglyphis*. Via this tract, among others, visual information from the BUs of the LX is transferred to the CX as has been demonstrated in various insects (el Jundi et al., 2014; Homberg et al., 2011; Schmitt, Stieb, et al., 2016; Sun et al., 2017). The overall layout of the CX in *Cataglyphis* (Figures 1 and 4) appears similar to other insect species such as dung beetles (el Jundi et al., 2018; Immonen et al., 2017), bees (Brandt et al., 2005; Pfeiffer & Kinoshita, 2012), *Drosophila* (Ito et al., 2014; Pereanu et al., 2010), monarch butterflies (Heinze et al., 2013), and locusts (Heinze, Gotthardt, & Homberg, 2009; von Hadeln et al., 2018). Future studies using additional markers and single neuron labeling are needed to reveal the fine structure of the different components of the CX. However, the prominent input from the sky-compass system and similarities in general layout are highly suggestive for an important role of the CX in path integration in *Cataglyphis* ants, especially in the light of recent studies on the neuronal network that encodes the current and desired directions in the CX network (Seelig & Jayaraman, 2015; Stone et al., 2017; Green, Vijayan, Pires, Adachi, & Maimon, 2019).

4.5 | Central adjoining neuropils

Even though the function of most areas within the CANP is largely unknown, the use of genetic tools in *Drosophila* promoted functional studies of the neuronal circuits in this brain region. For instance, novel calcium imaging tools in behaving flies could demonstrate the participation of different neuropils of the CANP in walking behavior (Aimon et al., 2019). To better relate and compare studies in other insects

with *Cataglyphis*, we subdivided the CANP into subunits using glial boundaries, fiber tracts, f-actin phalloidin staining as well as synapsin-ir and 5-HT-ir as criteria for defining borders. This first map of the CANP will allow us to study these brain regions in more detail in the future, particularly for investigating the distribution of neurotransmitters, neuromodulators, individual neurons and circuits, or gene expression profiles and compare these features directly with the situation in other insects.

Most of the described neuropils within the CANP of *Drosophila* do also exist in the brain of *Cataglyphis* (Figures 7 and 8). Since the enormous MBs of *Cataglyphis* occupy large parts of the central brain, the location and the size of the CANP components differ in some cases compared to the CANP in *Drosophila* and other insects investigated for this region so far. For instance, the CRE encases the complete ML of the MB in *Drosophila* (Ito et al., 2014) but appears much smaller and only around the tip of the ML in *Cataglyphis* (Figure 7h,i). Nevertheless, the general layout and location of the CANP components in *Cataglyphis* are very similar to other insects and appear as diverse as in dung beetles, fruit flies, locusts, and monarch butterflies (Heinze & Reppert, 2012; Immonen et al., 2017; Ito et al., 2014; von Hadeln et al., 2018). However, due to the lack of clear landmarks, we did not further subdivide some brain areas within the CANP of *Cataglyphis*. This concerns the CL, the PS, the ventrolateral complex (VX), and the VLP. Using the present template as a basis, the use of more diverse molecular markers might open up new insight into subdivisions in the future.

Our anterograde staining highlighted some subdivisions of the CANP in *Cataglyphis*, which largely correspond with previous investigations in other Hymenoptera (Zube et al., 2008; reviewed by: Galizia & Rössler, 2010; Rössler & Zube, 2011) and *Drosophila* (Tanaka, Endo, & Ito, 2012; Tanaka, Suzuki, Dye, Ejima, & Stopfer, 2012). Thus, the LH, the SIP (referred as "ring neuropil" in previous studies) and the VLNP receive olfactory information from the ALs (Figure 6). In addition, the VLNP and the VMNP receive visual input from the OLs (Figures 12a–g, 13, and 14), which is consistent with data from honey bees (Hertel & Maronde, 1987; Maronde, 1991; Milde, 1988), bumblebees (Paulk, Phillips-Portillo, Dacks, Fellous, & Gronenberg, 2008), and *Drosophila* (Namiki, Dickinson, Wong, Korff, & Card, 2018; Otsuna & Ito, 2006; Panser et al., 2016; Strausfeld, 1976; Wu et al., 2016). In flies, both brain regions are associated with the detection of directed motion and looming of objects (Ibbotson, Maddess, & DuBois, 1991; Klapoetke et al., 2017; Okamura & Strausfeld, 2007; Wicklein & Strausfeld, 2000; Wu et al., 2016). These very conserved findings across species illustrate the importance and behavioral relevance of distinct CANP structures as high-order integration centers in the insect brain.

4.6 | Visual projections in *Cataglyphis*

We confirmed two major optical tracts and four optic commissures in *Cataglyphis*. The anteriormost tract is the AOT (Figure 12a–c, 13, and 14a). The AOT seems to be a most conserved optic tract in insects. It

has been described in diverse insect orders such as Blattodea (Reischig & Stengl, 2002; Rosner et al., 2017), Coleoptera (Immonen et al., 2017), Diptera (Adden et al., 2019; Fischbach & Lyly-Hünerberg, 1983; Omoto et al., 2017; Power, 1943; Strausfeld, 1976), Lepidoptera (Collett, 1972; Strausfeld & Blest, 1970), Orthoptera (Homberg et al., 2003; Pfeiffer et al., 2005), and Hymenoptera including different *Cataglyphis* species (Grob et al., 2017; Held et al., 2016; Mota et al., 2011; Pfeiffer & Kinoshita, 2012; Schmitt, Stieb, et al., 2016). The AOT relays optic motion information (Collett, 1972; DeVoe et al., 1982; Paulk et al., 2008) as well as chromatic and polarization cues (Kinoshita et al., 2007; Mota et al., 2011; Pfeiffer et al., 2005) to the AOTU. In *Cataglyphis*, the AOT consists of projection neurons from the ME and LO (Figure 12a–c). Surprisingly, we also found that a few isolated neurons accompany the AOT but arborize into the VX instead of the AOTU (Figure 12g). Whether these neurons transmit similar information or completely different visual properties than other AOT-neurons requires future functional studies.

The OCT exclusively projects into the ipsilateral COs in the *Cataglyphis* brain (Figures 12a–c, 13, and 14a). To our knowledge, this tract has not been described before in any insect. Three different optic tracts, the ASOT, the anterior inferior optic tract (AIOT) and the LO tract (LOT) are known in honey bees (Ehmer & Gronenberg, 2002; Mobbs, 1984). In *Cataglyphis*, we did not find any evidence for a distinct AIOT or LOT. Instead, a very small subset of LO neurons join the ASOT formed by dorsal and ventral medullar neurons (Grob et al., 2017) and project into the calyces of both hemispheres (Figure 14b). The ASOT has exclusively been described in Hymenoptera, whereas other insects possess a prominent anterior optical commissure that we could not find in *Cataglyphis*—the great commissure (GC) (Immonen et al., 2017; Ito et al., 2014; Strausfeld, 1976; von Hadeln et al., 2018).

We also identified a commissure that exclusively interconnects the OLs in the *Cataglyphis* brain—the SOC (Figures 12a–c,h, 13, and 14b), which has previously been described in the brains of the cockroach *Leucophaea maderae* (Loesel & Homberg, 2001; Reischig & Stengl, 2002), crickets (Honegger & Schürmann, 1975; Tomioka, Nakamichi, & Yukizane, 1994) and the honey bee (Hertel & Maronde, 1987). In all of these insects, the SOC comprises only very few neurons originating from the LO and ME, which is consistent with our findings in *Cataglyphis* (Figure 12a–c). These neurons might respond to moving objects and play a role in tracking of objects as it has been shown in other insects (Hertel & Maronde, 1987; Loesel & Homberg, 2001).

The POC and the IOC are situated more posteriorly in the *Cataglyphis* brain. Here, the POC is a very prominent commissure. It was described in numerous insect species including Hymenoptera (Hertel & Maronde, 1987; Honegger & Schürmann, 1975; Immonen et al., 2017; Ito et al., 2014; Reischig & Stengl, 2002; von Hadeln et al., 2018; Yilmaz et al., 2016). In contrast, the IOC has only been described in few insect species such as the cockroach *Leucophaea maderae* (Reischig & Stengl, 2002), crickets (Honegger & Schürmann, 1975), and Hymenoptera (Hertel & Maronde, 1987; Mobbs, 1984; Paulk et al., 2008; Yilmaz et al., 2016). These tracts transfer, among others, information from the OL to the VMNPs and

the VLNPs. Electrophysiological recordings in bees showed that these neurons, for the most part, are achromatic (Hertel & Maronde, 1987; Paulk, Dacks, Phillips-Portillo, Fellous, & Gronenberg, 2009). Further results associated the neurons of the POC with the localization of stationary targets, while the IOC neurons respond to directional movements of objects (Hertel & Maronde, 1987; Maronde, 1991).

CONFLICT OF INTEREST

The authors declare no conflicts of interest.

AUTHOR CONTRIBUTIONS

Wolfgang Rössler, Basil el Jundi, Jens Habenstein, and Emad Amini contributed to study concept and design. Emad Amini, Kornelia Grübel, and Jens Habenstein contributed to preparation and acquisition of data. Jens Habenstein contributed to drafting of the manuscript. Emad Amini, Basil el Jundi, and Wolfgang Rössler contributed to critical review of the manuscript. Wolfgang Rössler obtained funding. All authors contributed to analyses and interpretation of data, and approved the final version of the manuscript for submission.

DATA AVAILABILITY STATEMENT

Three-dimensional data of the brain of Cataglyphis nodus are available at the Insect Brain Database website (https://www.insectbraindb.org/).

REFERENCES

Abel, R., Rybak, J., & Menzel, R. (2001). Structure and response patterns of olfactory interneurons in the honeybee, *Apis mellifera*. *Journal of Comparative Neurology*, 437(3), 363–383.

Adden, A., Wibrand, S., Pfeiffer, K., Warrant, E., & Heinze, S. (2020). The brain of a nocturnal migratory insect, the Australian Bogong moth. *Journal of Comparative Neurology*. https://doi.org/10.1002/cne.24866

Agosti, D. (1990). Review and reclassification of Cataglyphis (Hymenoptera, Formicidae). *Journal of Natural History*, 24(6), 1457–1505.

Ai, H., Nishino, H., & Itoh, T. (2007). Topographic organization of sensory afferents of Johnston's organ in the honeybee brain. *Journal of Comparative Neurology*, 502(6), 1030–1046.

Aimon, S., Katsuki, T., Jia, T., Grosenick, L., Broxton, M., Deisseroth, K., … Greenspan, R. J. (2019). Fast near–whole–brain imaging in adult

Drosophila during responses to stimuli and behavior. *PLoS Biology*, *17*(2), e2006732.

Brandt, R., Rohlfing, T., Rybak, J., Krofczik, S., Maye, A., Westerhoff, M., ... Menzel, R. (2005). Three-dimensional average-shape atlas of the honeybee brain and its applications. *Journal of Comparative Neurology*, *492*(1), 1–19.

Bressan, J., Benz, M., Oettler, J., Heinze, J., Hartenstein, V., & Sprecher, S. G. (2015). A map of brain neuropils and fiber systems in the ant Cardiocondyla obscurior. *Frontiers in Neuroanatomy*, *8*, 166.

Brill, M. F., Rosenbaum, T., Reus, I., Kleineidam, C. J., Nawrot, M. P., & Rössler, W. (2013). Parallel processing via a dual olfactory pathway in the honeybee. *Journal of Neuroscience*, *33*(6), 2443–2456.

Brill, M. F., Meyer, A., & Rössler, W. (2015). It takes two—Coincidence coding within the dual olfactory pathway of the honeybee. *Frontiers in Physiology*, *6*, 208.

Buehlmann, C., Graham, P., Hansson, B. S., & Knaden, M. (2014). Desert ants locate food by combining high sensitivity to food odors with extensive crosswind runs. *Current Biology*, *24*(9), 960–964.

Carcaud, J., Giurfa, M., & Sandoz, J.-C. (2015). Differential combinatorial coding of pheromones in two olfactory subsystems of the honey bee brain. *Journal of Neuroscience*, *35*(10), 4157–4167.

Collett, T. (1972). Visual neurones in the anterior optic tract of the privet hawk moth. *Journal of Comparative Physiology*, *78*(4), 396–433.

Collett, T. S., Dillmann, E., Giger, A., & Wehner, R. (1992). Visual landmarks and route following in desert ants. *Journal of Comparative Physiology A*, *170*(4), 435–442.

Couto, A., Lapeyre, B., Thiéry, D., & Sandoz, J. C. (2016). Olfactory pathway of the hornet Vespa velutina: New insights into the evolution of the hymenopteran antennal lobe. *Journal of Comparative Neurology*, *524*(11), 2335–2359.

Cruse, H., & Wehner, R. (2011). No need for a cognitive map: Decentralized memory for insect navigation. *PLoS Computational Biology*, *7*(3), e1002009.

Dacks, A. M., Christensen, T. A., & Hildebrand, J. G. (2006). Phylogeny of a serotonin-immunoreactive neuron in the primary olfactory center of the insect brain. *Journal of Comparative Neurology*, *498*(6), 727–746.

Dancker, P., Low, I., Hasselbach, W., & Wieland, T. (1975). Interaction of Actin with phalloidin: Polymerization and stabilization of F-Actin. *Biochimica et Biophysica Acta*, *400*(2), 407–414.

Dettner, K., & Peters, W. (2011). *Lehrbuch der Entomologie*. Heidelberg: Springer Spektrum.

DeVoe, R. D., Kaiser, W., Ohm, J., & Stone, L. S. (1982). Horizontal movement detectors of honeybees: Directionally-selective visual neurons in the lobula and brain. *Journal of Comparative Physiology*, *147*(2), 155–170.

Ehmer, B., & Gronenberg, W. (1997). Proprioceptors and fast antennal reflexes in the ant Odontomachus (Formicidae, Ponerinae). *Cell and Tissue Research*, *290*(1), 153–165.

Ehmer, B., & Gronenberg, W. (2002). Segregation of visual input to the mushroom bodies in the honeybee (*Apis mellifera*). *Journal of Comparative Neurology*, *451*(4), 362–373.

Ehmer, B., & Gronenberg, W. (2004). Mushroom body volumes and visual interneurons in ants: Comparison between sexes and castes. *Journal of Comparative Neurology*, *469*(2), 198–213.

el Jundi, B., Huetteroth, W., Kurylas, A. E., & Schachtner, J. (2009). Anisometric brain dimorphism revisited: Implementation of a volumetric 3D standard brain in Manduca sexta. *Journal of Comparative Neurology*, *517*(2), 210–225.

el Jundi, B., Heinze, S., Lenschow, C., Kurylas, A., Rohlfing, T., & Homberg, U. (2010). The locust standard brain: A 3D standard of the central complex as a platform for neural network analysis. *Frontiers in Systems Neuroscience*, *3*, 21.

el Jundi, B., & Homberg, U. (2010). Evidence for the possible existence of a second polarization-vision pathway in the locust brain. *Journal of Insect Physiology*, *56*(8), 971–979.

el Jundi, B., Pfeiffer, K., & Homberg, U. (2011). A distinct layer of the medulla integrates sky compass signals in the brain of an insect. *PLoS One*, *6*(11), e27855.

el Jundi, B., & Homberg, U. (2012). Receptive field properties and intensity-response functions of polarization-sensitive neurons of the optic tubercle in gregarious and solitarious locusts. *Journal of Neurophysiology*, *108*(6), 1695–1710.

el Jundi, B., Pfeiffer, K., Heinze, S., & Homberg, U. (2014). Integration of polarization and chromatic cues in the insect sky compass. *Journal of Comparative Physiology A*, *200*(6), 575–589.

el Jundi, B., Warrant, E. J., Pfeiffer, K., & Dacke, M. (2018). Neuroarchitecture of the dung beetle central complex. *Journal of Comparative Neurology*, *526*(16), 2612–2630.

Erber, J., Masuhr, T., & Menzel, R. (1980). Localization of short-term memory in the brain of the bee, *Apis mellifera*. *Physiological Entomology*, *5*(4), 343–358.

Fahrbach, S. E. (2006). Structure of the mushroom bodies of the insect brain. *Annual Review of Entomology*, *51*, 209–232.

Falibene, A., Rössler, W., & Josens, R. (2012). Serotonin depresses feeding behaviour in ants. *Journal of Insect Physiology*, *58*(1), 7–17.

Farris, S. M. (2005). Evolution of insect mushroom bodies: Old clues, new insights. *Arthropod Structure & Development*, *34*(3), 211–234.

Farris, S. M. (2008). Tritocerebral tract input to the insect mushroom bodies. *Arthropod Structure & Development*, *37*(6), 492–503.

Farris, S. M., & Schulmeister, S. (2010). Parasitoidism, not sociality, is associated with the evolution of elaborate mushroom bodies in the brains of hymenopteran insects. *Proceedings of the Royal Society B: Biological Sciences*, *278*(1707), 940–951.

Farris, S. M. (2013). Evolution of complex higher brain centers and behaviors: Behavioral correlates of mushroom body elaboration in insects. *Brain, Behavior and Evolution*, *82*(1), 9–18.

Farris, S. M. (2015). Evolution of brain elaboration. *Philosophical Transactions of the Royal Society B: Biological Sciences*, *370*(1684), 20150054.

Fischbach, K., & Lyly-Hünerberg, I. (1983). Genetic dissection of the anterior optic tract of *Drosophila melanogaster*. *Cell and Tissue Research*, *231*(3), 551–563.

Fleischmann, P. N., Christian, M., Müller, V. L., Rössler, W., & Wehner, R. (2016). Ontogeny of learning walks and the acquisition of landmark information in desert ants, *Cataglyphis fortis*. *Journal of Experimental Biology*, *219*(19), 3137–3145.

Fleischmann, P. N., Grob, R., Wehner, R., & Rössler, W. (2017). Species-specific differences in the fine structure of learning walk elements in Cataglyphis ants. *Journal of Experimental Biology*, *220*(13), 2426–2435.

Fleischmann, P. N., Grob, R., Müller, V. L., Wehner, R., & Rössler, W. (2018). The geomagnetic field is a compass cue in Cataglyphis ant navigation. *Current Biology*, *28*(9), 1440, e1442–1444.

Frambach, I., Rössler, W., Winkler, M., & Schurmann, F. W. (2004). F-Actin at identified synapses in the mushroom body neuropil of the insect brain. *Journal of Comparative Neurology*, *475*(3), 303–314.

Galizia, C. G., & Rössler, W. (2010). Parallel olfactory systems in insects: Anatomy and function. *Annual Review of Entomology*, *55*, 399–420.

Green, J., Vijayan, V., Pires, P. M., Adachi, A., & Maimon, G. (2019). A neural heading estimate is compared with an internal goal to guide oriented navigation. *Nature Neuroscience*, *22*(9), 1460–1468.

Grob, R., Fleischmann, P. N., Grübel, K., Wehner, R., & Rössler, W. (2017). The role of celestial compass information in Cataglyphis ants during learning walks and for neuroplasticity in the central complex and mushroom bodies. *Frontiers in Behavioral Neuroscience*, *11*, 226.

Grob, R., Fleischmann, P. N., & Rössler, W. (2019). Learning to navigate–how desert ants calibrate their compass systems. *E-Neuroforum*, *25*(2), 109–120.

Groh, C., & Rössler, W. (2011). Comparison of microglomerular structures in the mushroom body calyx of neopteran insects. *Arthropod Structure & Development*, *40*(4), 358–367.

Groh, C., Kelber, C., Grübel, K., & Rössler, W. (2014). Density of mushroom body synaptic complexes limits intraspecies brain miniaturization in highly polymorphic leaf-cutting ant workers. *Proceedings of the Royal Society B: Biological Sciences*, *281*(1785), 20140432.

Groh, C., & Rössler, W. (2020). Analysis of synaptic microcircuits in the mushroom bodies of the honeybee. *Insects*, *11*(1), 43.

Gronenberg, W. (1999). Modality-specific segregation of input to ant mushroom bodies. *Brain, Behavior and Evolution*, *54*(2), 85–95.

Gronenberg, W., & Hölldobler, B. (1999). Morphologic representation of visual and antennal information in the ant brain. *Journal of Comparative Neurology*, *412*(2), 229–240.

Gronenberg, W. (2001). Subdivisions of hymenopteran mushroom body calyces by their afferent supply. *Journal of Comparative Neurology*, *435*(4), 474–489.

Gronenberg, W. (2008). Structure and function of ant (hymenoptera: Formicidae) brains: Strength in numbers. *Myrmecological News*, *11*, 25–36.

Groothuis, J., Pfeiffer, K., el Jundi, B., & Smid, H. M. (2019). The Jewel wasp standard brain: Average shape atlas and morphology of the female Nasonia vitripennis brain. *Arthropod Structure & Development*, *51*, 41–51.

Grünewald, B. (1999). Physiological properties and response modulations of mushroom body feedback neurons during olfactory learning in the honeybee, *Apis mellifera*. *Journal of Comparative Physiology A*, *185*(6), 565–576.

Guo, P., & Ritzmann, R. E. (2013). Neural activity in the central complex of the cockroach brain is linked to turning behaviors. *Journal of Experimental Biology*, *216*(6), 992–1002.

Haehnel, M., & Menzel, R. (2010). Sensory representation and learning-related plasticity in mushroom body extrinsic feedback neurons of the protocerebral tract. *Frontiers in Systems Neuroscience*, *4*, 161.

Hausen, K. (1976). Functional characterization and anatomical identification of motion sensitive neurons in the lobula plate of the blowfly Calliphora erythrocephala. *Zeitschrift für Naturforschung c*, *31*(9–10), 629–634.

Hausen, K. (1984). The lobula-complex of the fly: Structure, function and significance in visual behaviour. In *Photoreception and vision in invertebrates* (pp. 523–559). Berlin, Heidelberg: Springer.

Heinze, S., & Homberg, U. (2007). Maplike representation of celestial E-vector orientations in the brain of an insect. *Science*, *315*(5814), 995–997.

Heinze, S., & Homberg, U. (2008). Neuroarchitecture of the central complex of the desert locust: Intrinsic and columnar neurons. *Journal of Comparative Neurology*, *511*(4), 454–478.

Heinze, S., Gotthardt, S., & Homberg, U. (2009). Transformation of polarized light information in the central complex of the locust. *Journal of Neuroscience*, *29*(38), 11783–11793.

Heinze, S., & Reppert, S. M. (2011). Sun compass integration of skylight cues in migratory monarch butterflies. *Neuron*, *69*(2), 345–358.

Heinze, S., & Reppert, S. M. (2012). Anatomical basis of sun compass navigation I: The general layout of the monarch butterfly brain. *Journal of Comparative Neurology*, *520*(8), 1599–1628.

Heinze, S., Florman, J., Asokaraj, S., El Jundi, B., & Reppert, S. M. (2013). Anatomical basis of sun compass navigation II: The neuronal composition of the central complex of the monarch butterfly. *Journal of Comparative Neurology*, *521*(2), 267–298.

Heinze, S. (2014). Polarized-light processing in insect brains: recent insights from the desert locust, the monarch butterfly, the cricket, and the fruit fly. In *Polarized light and polarization vision in animal sciences* (pp. 61–111). Berlin, Heidelberg: Springer.

Heisenberg, M. (2003). Mushroom body memoir: From maps to models. *Nature Reviews Neuroscience*, *4*(4), 266–275.

Held, M., Berz, A., Hensgen, R., Muenz, T. S., Scholl, C., Rössler, W., ... Pfeiffer, K. (2016). Microglomerular synaptic complexes in the sky-compass network of the honeybee connect parallel pathways from the anterior optic tubercle to the central complex. *Frontiers in Behavioral Neuroscience*, *10*, 186.

Hertel, H., Schäfer, S., & Maronde, U. (1987). The physiology and morphology of visual commissures in the honeybee brain. *Journal of Experimental Biology*, *133*(1), 283–300.

Hertel, H., & Maronde, U. (1987). Processing of visual information in the honeybee brain. In *Neurobiology and behavior of honeybees* (pp. 141–157). Berlin, Heidelberg: Springer.

Hofbauer, A., Ebel, T., Waltenspiel, B., Oswald, P., Chen, Y.-C., Halder, P., ... Buchner, E. (2009). The Wuerzburg hybridoma library against drosophila brain. *Journal of Neurogenetics*, *23*(1–2), 78–91.

Hölldobler, B., & Wilson, E. O. (1990). *The ants*. Berlin, Heidelberg: Springer-Verlag.

Homberg, U., Christensen, T. A., & Hildebrand, J. G. (1989). Structure and function of the deutocerebrum in insects. *Annual Review of Entomology*, *34*(1), 477–501.

Homberg, U., Hofer, S., Pfeiffer, K., & Gebhardt, S. (2003). Organization and neural connections of the anterior optic tubercle in the brain of the locust, Schistocerca gregaria. *Journal of Comparative Neurology*, *462*(4), 415–430.

Homberg, U. (2004). In search of the sky compass in the insect brain. *Naturwissenschaften*, *91*(5), 199–208.

Homberg, U., Heinze, S., Pfeiffer, K., Kinoshita, M., & el Jundi, B. (2011). Central neural coding of sky polarization in insects. *Philosophical Transactions of the Royal Society B*, *366*(1565), 680–687.

Honegger, H.-W., & Schürmann, F. (1975). Cobalt sulphide staining of optic fibres in the brain of the cricket, Gryllus campestris. *Cell and Tissue Research*, *159*(2), 213–225.

Hoyer, S. C., Liebig, J., & Rössler, W. (2005). Biogenic amines in the ponerine ant *Harpegnathos saltator*: Serotonin and dopamine immunoreactivity in the brain. *Arthropod Structure & Development*, *34*(4), 429–440.

Huber, R., & Knaden, M. (2015). Egocentric and geocentric navigation during extremely long foraging paths of desert ants. *Journal of Comparative Physiology A*, *201*(6), 609–616.

Huetteroth, W., El Jundi, B., El Jundi, S., & Schachtner, J. (2010). 3D-reconstructions and virtual 4D-visualization to study metamorphic brain development in the sphinx moth Manduca sexta. *Frontiers in Systems Neuroscience*, *4*, 7.

Ibbotson, M., Maddess, T., & DuBois, R. (1991). A system of insect neurons sensitive to horizontal and vertical image motion connects the medulla and midbrain. *Journal of Comparative Physiology A*, *169*(3), 355–367.

Ilieş, I., Muscedere, M. L., & Traniello, J. F. (2015). Neuroanatomical and morphological trait clusters in the ant genus Pheidole: Evidence for modularity and integration in brain structure. *Brain, Behavior and Evolution*, *85*(1), 63–76.

Immonen, E. V., Dacke, M., Heinze, S., & el Jundi, B. (2017). Anatomical organization of the brain of a diurnal and a nocturnal dung beetle. *Journal of Comparative Neurology*, *525*(8), 1879–1908.

Ito, K., Shinomiya, K., Ito, M., Armstrong, J. D., Boyan, G., Hartenstein, V., ... Vosshall, L. B. (2014). A systematic nomenclature for the insect brain. *Neuron*, *81*(4), 755–765.

Joesch, M., Plett, J., Borst, A., & Reiff, D. F. (2008). Response properties of motion-sensitive visual interneurons in the lobula plate of *Drosophila melanogaster*. *Current Biology*, *18*(5), 368–374.

Jørgensen, K., Kvello, P., Almaas, T. J., & Mustaparta, H. (2006). Two closely located areas in the suboesophageal ganglion and the tritocerebrum receive projections of gustatory receptor neurons located on the antennae and the proboscis in the moth Heliothis virescens. *Journal of Comparative Neurology*, *496*(1), 121–134.

Kamikouchi, A., Inagaki, H. K., Effertz, T., Hendrich, O., Fiala, A., Göpfert, M. C., & Ito, K. (2009). The neural basis of drosophila gravity-sensing and hearing. *Nature*, *458*(7235), 165–171.

Kelber, C., Rössler, W., Roces, F., & Kleineidam, C. J. (2009). The antennal lobes of fungus-growing ants (Attini): Neuroanatomical traits and evolutionary trends. *Brain, Behavior and Evolution*, *73*(4), 273–284.

26 | WILEY—JCN | HABENSTEIN ET AL.

Kinoshita, M., Pfeiffer, K., & Homberg, U. (2007). Spectral properties of identified polarized-light sensitive interneurons in the brain of the desert locust Schistocerca gregaria. *Journal of Experimental Biology*, *210*(8), 1350–1361.

Kirkhart, C., & Scott, K. (2015). Gustatory learning and processing in the drosophila mushroom bodies. *Journal of Neuroscience*, *35*(15), 5950–5958.

Kirschner, S., Kleineidam, C. J., Zube, C., Rybak, J., Grünewald, B., & Rössler, W. (2006). Dual olfactory pathway in the honeybee, *Apis mellifera*. *Journal of Comparative Neurology*, *499*(6), 933–952.

Klagges, B. R., Heimbeck, G., Godenschwege, T. A., Hofbauer, A., Pflugfelder, G. O., Reifegerste, R., ... Buchner, E. (1996). Invertebrate synapsins: A single gene codes for several isoforms in drosophila. *Journal of Neuroscience*, *16*(10), 3154–3165.

Klapoetke, N. C., Nern, A., Peek, M. Y., Rogers, E. M., Breads, P., Rubin, G. M., ... Card, G. M. (2017). Ultra-selective looming detection from radial motion opponency. *Nature*, *551*(7679), 237–241.

Knaden, M., & Wehner, R. (2005). Nest mark orientation in desert ants Cataglyphis: What does it do to the path integrator? *Animal Behaviour*, *70*(6), 1349–1354.

Kurylas, A. E., Rohlfing, T., Krofczik, S., Jenett, A., & Homberg, U. (2008). Standardized atlas of the brain of the desert locust, Schistocerca gregaria. *Cell and Tissue Research*, *333*(1), 125–145.

Laissue, P., Reiter, C., Hiesinger, P., Halter, S., Fischbach, K., & Stocker, R. (1999). Three-dimensional reconstruction of the antennal lobe in *Drosophila melanogaster*. *Journal of Comparative Neurology*, *405*(4), 543–552.

Lebhardt, F., & Ronacher, B. (2014). Interactions of the polarization and the sun compass in path integration of desert ants. *Journal of Comparative Physiology A*, *200*(8), 711–720.

Lebhardt, F., & Ronacher, B. (2015). Transfer of directional information between the polarization compass and the sun compass in desert ants. *Journal of Comparative Physiology A*, *201*(6), 599–608.

Li, Y., & Strausfeld, N. J. (1997). Morphology and sensory modality of mushroom body extrinsic neurons in the brain of the cockroach, *Periplaneta americana*. *Journal of Comparative Neurology*, *387*(4), 631–650.

Lin, H.-H., Lai, J. S.-Y., Chin, A.-L., Chen, Y.-C., & Chiang, A.-S. (2007). A map of olfactory representation in the drosophila mushroom body. *Cell*, *128*(6), 1205–1217.

Liu, L., Wolf, R., Ernst, R., & Heisenberg, M. (1999). Context generalization in drosophila visual learning requires the mushroom bodies. *Nature*, *400*(6746), 753.

Loesel, R., & Homberg, U. (2001). Anatomy and physiology of neurons with processes in the accessory medulla of the cockroach *Leucophaea maderae*. *Journal of Comparative Neurology*, *439*(2), 193–207.

Maronde, U. (1991). Common projection areas of antennal and visual pathways in the honeybee brain, *Apis mellifera*. *Journal of Comparative Neurology*, *309*(3), 328–340.

Martin, J. P., Guo, P., Mu, L., Harley, C. M., & Ritzmann, R. E. (2015). Central-complex control of movement in the freely walking cockroach. *Current Biology*, *25*(21), 2795–2803.

Masante-Roca, I., Gadenne, C., & Anton, S. (2005). Three-dimensional antennal lobe atlas of male and female moths, Lobesia botrana (Lepidoptera: Tortricidae) and glomerular representation of plant volatiles in females. *Journal of Experimental Biology*, *208*(6), 1147–1159.

Menzel, R. (1999). Memory dynamics in the honeybee. *Journal of Comparative Physiology A*, *185*(4), 323–340.

Menzel, R. (2001). Searching for the memory trace in a mini-brain, the honeybee. *Learning & Memory*, *8*(2), 53–62.

Menzel, R. (2014). The insect mushroom body, an experience-dependent recoding device. *Journal of Physiology*, *108*(2–3), 84–95.

Milde, J. J. (1988). Visual responses of interneurones in the posterior median protocerebrum and the central complex of the honeybee *Apis mellifera*. *Journal of Insect Physiology*, *34*(5), 427–436.

Miyazaki, T., & Ito, K. (2010). Neural architecture of the primary gustatory center of *Drosophila melanogaster* visualized with GAL4 and LexA enhancer-trap systems. *Journal of Comparative Neurology*, *518*(20), 4147–4181.

Mobbs, P. (1982). The brain of the honeybee *Apis mellifera*. I. the connections and spatial organization of the mushroom bodies. *Philosophical Transactions of the Royal Society of London B, Biological Sciences*, *298*(1091), 309–354.

Mobbs, P. (1984). Neural networks in the mushroom bodies of the honeybee. *Journal of Insect Physiology*, *30*(1), 43–58.

Montgomery, S. H., & Ott, S. R. (2015). Brain composition in Godyris zavaleta, a diurnal butterfly, reflects an increased reliance on olfactory information. *Journal of Comparative Neurology*, *523*(6), 869–891.

Montgomery, S. H., Merrill, R. M., & Ott, S. R. (2016). Brain composition in Heliconius butterflies, posteclosion growth and experience-dependent neuropil plasticity. *Journal of Comparative Neurology*, *524*(9), 1747–1769.

Mota, T., Yamagata, N., Giurfa, M., Gronenberg, W., & Sandoz, J.-C. (2011). Neural organization and visual processing in the anterior optic tubercle of the honeybee brain. *Journal of Neuroscience*, *31*(32), 11443–11456.

Mota, T., Gronenberg, W., Giurfa, M., & Sandoz, J.-C. (2013). Chromatic processing in the anterior optic tubercle of the honey bee brain. *Journal of Neuroscience*, *33*(1), 4–16.

Mota, T., Kreissl, S., Carrasco, D. A., Lefer, D., Galizia, G., & Giurfa, M. (2016). Synaptic organization of microglomerular clusters in the lateral and medial bulbs of the honeybee brain. *Frontiers in Neuroanatomy*, *10*, 103.

Müller, D., Abel, R., Brandt, R., Zöckler, M., & Menzel, R. (2002). Differential parallel processing of olfactory information in the honeybee, *Apis mellifera* L. *Journal of Comparative Physiology A*, *188*(5), 359–370.

Müller, M., & Wehner, R. (1988). Path integration in desert ants, *Cataglyphis fortis*. *Proceedings of the National Academy of Science of the USA*, *85*(14), 5287–5290.

Namiki, S., & Kanzaki, R. (2016). Comparative neuroanatomy of the lateral accessory lobe in the insect brain. *Frontiers in Physiology*, *7*, 244.

Namiki, S., Dickinson, M. H., Wong, A. M., Korff, W., & Card, G. M. (2018). The functional organization of descending sensory-motor pathways in drosophila. *Elife*, *7*, e34272.

Nishikawa, M., Nishino, H., Misaka, Y., Kubota, M., Tsuji, E., Satoji, Y., ... Yokohari, F. (2008). Sexual dimorphism in the antennal lobe of the ant *Camponotus japonicus*. *Zoological Science*, *25*(2), 195–205.

Okamura, J. Y., & Strausfeld, N. J. (2007). Visual system of calliphorid flies: Motion-and orientation-sensitive visual interneurons supplying dorsal optic glomeruli. *Journal of Comparative Neurology*, *500*(1), 189–208.

Omoto, J. J., Keleş, M. F., Nguyen, B.-C. M., Bolanos, C., Lovick, J. K., Frye, M. A., & Hartenstein, V. (2017). Visual input to the drosophila central complex by developmentally and functionally distinct neuronal populations. *Current Biology*, *27*(8), 1098–1110.

Otsuna, H., & Ito, K. (2006). Systematic analysis of the visual projection neurons of *Drosophila melanogaster*. I. Lobula-specific pathways. *Journal of Comparative Neurology*, *497*(6), 928–958.

Panser, K., Tirian, L., Schulze, F., Villalba, S., Jefferis, G. S., Buehler, K., & Straw, A. D. (2016). Automatic segmentation of Drosophila neural compartments using GAL4 expression data reveals novel visual pathways. *Current Biology*, *26*(15), 1943–1954.

Pasch, E., Muenz, T. S., & Rössler, W. (2011). CaMKII is differentially localized in synaptic regions of Kenyon cells within the mushroom bodies of the honeybee brain. *Journal of Comparative Neurology*, *519*(18), 3700–3712.

Paulk, A. C., Phillips-Portillo, J., Dacks, A. M., Fellous, J.-M., & Gronenberg, W. (2008). The processing of color, motion, and stimulus timing are anatomically segregated in the bumblebee brain. *Journal of Neuroscience*, *28*(25), 6319–6332.

Paulk, A. C., & Gronenberg, W. (2008). Higher order visual input to the mushroom bodies in the bee, *Bombus impatiens*. *Arthropod Structure & Development*, *37*(6), 443–458.

Paulk, A. C., Dacks, A. M., Phillips-Portillo, J., Fellous, J.-M., & Gronenberg, W. (2009). Visual processing in the central bee brain. *Journal of Neuroscience*, 29(32), 9987–9999.

Pereanu, W., Kumar, A., Jennett, A., Reichert, H., & Hartenstein, V. (2010). Development-based compartmentalization of the Drosophila central brain. *Journal of Comparative Neurology*, 518(15), 2996–3023.

Pfeffer, S. E., & Wittlinger, M. (2016). Optic flow odometry operates independently of stride integration in carried ants. *Science*, 353(6304), 1155–1157.

Pfeiffer, K., Kinoshita, M., & Homberg, U. (2005). Polarization-sensitive and light-sensitive neurons in two parallel pathways passing through the anterior optic tubercle in the locust brain. *Journal of Neurophysiology*, 94, 3903–3915.

Pfeiffer, K., & Homberg, U. (2007). Coding of azimuthal directions via time-compensated combination of celestial compass cues. *Current Biology*, 17(11), 960–965.

Pfeiffer, K., & Kinoshita, M. (2012). Segregation of visual inputs from different regions of the compound eye in two parallel pathways through the anterior optic tubercle of the bumblebee (*Bombus ignitus*). *Journal of Comparative Neurology*, 520(2), 212–229.

Power, M. E. (1943). The brain of *Drosophila melanogaster*. *Journal of Morphology*, 72(3), 517–559.

Preibisch, S., Saalfeld, S., & Tomancak, P. (2009). Globally optimal stitching of tiled 3D microscopic image acquisitions. *Bioinformatics*, 25(11), 1463–1465.

Reischig, T., & Stengl, M. (2002). Optic lobe commissures in a three-dimensional brain model of the cockroach *Leucophaea maderae*: A search for the circadian coupling pathways. *Journal of Comparative Neurology*, 443(4), 388–400.

Ribi, W., Senden, T. J., Sakellariou, A., Limaye, A., & Zhang, S. (2008). Imaging honey bee brain anatomy with micro-X-ray-computed tomography. *Journal of Neuroscience Methods*, 171(1), 93–97.

Ronacher, B. (2008). Path integration as the basic navigation mechanism of the desert ant *Cataglyphis fortis* (Forel, 1902) (Hymenoptera: Formicidae). *Myrmecological News*, 11, 53–62.

Rosner, R., von Hadeln, J., Salden, T., & Homberg, U. (2017). Anatomy of the lobula complex in the brain of the praying mantis compared to the lobula complexes of the locust and cockroach. *Journal of Comparative Neurology*, 525(10), 2343–2357.

Rössler, W., Kuduz, J., Schürmann, F. W., & Schild, D. (2002). Aggregation of F-actin in olfactory glomeruli: A common feature of glomeruli across phyla. *Chemical Senses*, 27(9), 803–810.

Rössler, W., & Zube, C. (2011). Dual olfactory pathway in hymenoptera: Evolutionary insights from comparative studies. *Arthropod Structure & Development*, 40(4), 349–357.

Rössler, W., & Groh, C. (2012). Plasticity of synaptic microcircuits in the mushroom-body calyx of the honey bee. In *Honeybee neurobiology and behavior* (pp. 141–153). Dordrecht, Heidelberg, London New York: Springer.

Rössler, W., & Brill, M. F. (2013). Parallel processing in the honeybee olfactory pathway: Structure, function, and evolution. *Journal of Comparative Physiology A*, 199(11), 981–996.

Rössler, W. (2019). Neuroplasticity in desert ants (hymenoptera: Formicidae)– importance for the ontogeny of navigation. *Myrmecological News*, 29, 1–20.

Ruano, F., Tinaut, A., & Soler, J. J. (2000). High surface temperatures select for individual foraging in ants. *Behavioral Ecology*, 11(4), 396–404.

Sancer, G., Kind, E., Plazaola-Sasieta, H., Balke, J., Pham, T., Hasan, A., … Wernet, M. F. (2019). Modality-specific circuits for skylight orientation in the fly visual system. *Current Biology*, 29(17), 2812–2825.

Schmeling, F., Tegtmeier, J., Kinoshita, M., & Homberg, U. (2015). Photoreceptor projections and receptive fields in the dorsal rim area and main retina of the locust eye. *Journal of Comparative Physiology A*, 201(5), 427–440.

Schmitt, F., Stieb, S. M., Wehner, R., & Rossler, W. (2016). Experience-related reorganization of giant synapses in the lateral complex: Potential role in plasticity of the sky-compass pathway in the desert ant *Cataglyphis fortis*. *Developmental Neurobiology*, 76(4), 390–404.

Schmitt, F., Vanselow, J. T., Schlosser, A., Wegener, C., & Rossler, W. (2016). Neuropeptides in the desert ant *Cataglyphis fortis*: Mass spectrometric analysis, localization, and age-related changes. *Journal of Comparative Neurology*, 525, 901–918.

Scholtz, G., & Edgecombe, G. D. (2006). The evolution of arthropod heads: Reconciling morphological, developmental and palaeontological evidence. *Development Genes and Evolution*, 216(7–8), 395–415.

Seelig, J. D., & Jayaraman, V. (2013). Feature detection and orientation tuning in the Drosophila central complex. *Nature*, 503(7475), 262.

Seelig, J. D., & Jayaraman, V. (2015). Neural dynamics for landmark orientation and angular path integration. *Nature*, 521(7551), 186.

Steck, K., Hansson, B. S., & Knaden, M. (2011). Desert ants benefit from combining visual and olfactory landmarks. *Journal of Experimental Biology*, 214(8), 1307–1312.

Stieb, S. M., Muenz, T. S., Wehner, R., & Rössler, W. (2010). Visual experience and age affect synaptic organization in the mushroom bodies of the desert ant *Cataglyphis fortis*. *Developmental Neurobiology*, 70(6), 408–423.

Stieb, S. M., Kelber, C., Wehner, R., & Rössler, W. (2011). Antennal-lobe organization in desert ants of the genus Cataglyphis. *Brain, Behavior and Evolution*, 77(3), 136–146.

Stieb, S. M., Hellwig, A., Wehner, R., & Rössler, W. (2012). Visual experience affects both behavioral and neuronal aspects in the individual life history of the desert ant *Cataglyphis fortis*. *Developmental Neurobiology*, 72(5), 729–742.

Stocker, R., Lienhard, M., Borst, A., & Fischbach, K. (1990). Neuronal architecture of the antennal lobe in *Drosophila melanogaster*. *Cell and Tissue Research*, 262(1), 9–34.

Stone, T., Webb, B., Adden, A., Weddig, N. B., Honkanen, A., Templin, R., … Heinze, S. (2017). An anatomically constrained model for path integration in the bee brain. *Current Biology*, 27(20), 3069–3085. e3011.

Strausfeld, N. J., & Blest, A. (1970). Golgi studies on insects Part I. The optic lobes of Lepidoptera. *Philosophical Transactions of the Royal Society of London B, Biological Sciences*, 258(820), 81–134.

Strausfeld N. J. (1976). *Atlas of an insect brain*. Berlin, Heidelberg, New York: Springer.

Strausfeld, N. J., Homburg, U., & Kloppenberg, P. (2000). Parallel organization in honey bee mushroom bodies by peptidergic Kenyon cells. *Journal of Comparative Neurology*, 424(1), 179–195.

Strausfeld, N. J. (2002). Organization of the honey bee mushroom body: Representation of the calyx within the vertical and gamma lobes. *Journal of Comparative Neurology*, 450(1), 4–33.

Strausfeld, N. J., & Okamura, J. Y. (2007). Visual system of calliphorid flies: Organization of optic glomeruli and their lobula complex efferents. *Journal of Comparative Neurology*, 500(1), 166–188.

Strausfeld, N. J., Sinakevitch, I., Brown, S. M., & Farris, S. M. (2009). Ground plan of the insect mushroom body: Functional and evolutionary implications. *Journal of Comparative Neurology*, 513(3), 265–291.

Strausfeld, N. J. (2012). *Arthropod brains: Evolution, functional elegance, and historical significance*. Cambridge, MA: Belknap Press of Harvard University Press.

Strauss, R. (2002). The central complex and the genetic dissection of locomotor behaviour. *Current Opinion in Neurobiology*, 12(6), 633–638.

Sun, Y., Nern, A., Franconville, R., Dana, H., Schreiter, E. R., Looger, L. L., … Jayaraman, V. (2017). Neural signatures of dynamic stimulus selection in Drosophila. *Nature Neuroscience*, 20(8), 1104–1113.

Szyszka, P., Galkin, A., & Menzel, R. (2008). Associative and non-associative plasticity in Kenyon cells of the honeybee mushroom body. *Frontiers in Systems Neuroscience*, 2, 3.

Tanaka, N. K., Tanimoto, H., & Ito, K. (2008). Neuronal assemblies of the Drosophila mushroom body. *Journal of Comparative Neurology*, 508(5), 711–755.

Tanaka, N. K., Suzuki, E., Dye, L., Ejima, A., & Stopfer, M. (2012). Dye fills reveal additional olfactory tracts in the protocerebrum of wild-type Drosophila. *Journal of Comparative Neurology*, 520(18), 4131–4140.

Tanaka, N. K., Endo, K., & Ito, K. (2012). Organization of antennal lobe-associated neurons in adult *Drosophila melanogaster* brain. *Journal of Comparative Neurology*, 520(18), 4067–4130.

Tomioka, K., Nakamichi, M., & Yukizane, M. (1994). Optic lobe circadian pacemaker sends its information to the contralateral optic lobe in the cricket Gryllus bimaculatus. *Journal of Comparative Physiology A*, 175(4), 381–388.

Träger, U., Wagner, R., Bausenwein, B., & Homberg, U. (2008). A novel type of microglomerular synaptic complex in the polarization vision pathway of the locust brain. *Journal of Comparative Neurology*, 506(2), 288–300.

Turner-Evans, D. B., & Jayaraman, V. (2016). The insect central complex. *Current Biology*, 26(11), R453–R457.

Varela, N., Couton, L., Gemeno, C., Avilla, J., Rospars, J.-P., & Anton, S. (2009). Three-dimensional antennal lobe atlas of the oriental fruit moth, Cydia molesta (Busck) (Lepidoptera: Tortricidae): Comparison of male and female glomerular organization. *Cell and Tissue Research*, 337(3), 513–526.

von Hadeln, J., Althaus, V., Häger, L., & Homberg, U. (2018). Anatomical organization of the cerebrum of the desert locust Schistocerca gregaria. *Cell and Tissue Research*, 374(1), 39–62.

Warren, T. L., Giraldo, Y. M., & Dickinson, M. H. (2019). Celestial navigation in Drosophila. *Journal of Experimental Biology*, 222(Suppl 1), jeb186148.

Watanabe, H., Shimohigashi, M., & Yokohari, F. (2014). Serotonin-immunoreactive sensory neurons in the antenna of the cockroach Periplaneta americana. *Journal of Comparative Neurology*, 522(2), 414–434.

Wehner, R., & Menzel, R. (1969). Homing in the ant *Cataglyphis bicolor*. *Science*, 164(3876), 192–194.

Wehner, R., & Räber, F. (1979). Visual spatial memory in desert ants, *Cataglyphis bicolor* (Hymenoptera: Formicidae). *Experientia*, 35(12), 1569–1571.

Wehner, R., Michel, B., & Antonsen, P. (1996). Visual navigation in insects: Coupling of egocentric and geocentric information. *Journal of Experimental Biology*, 199(1), 129–140.

Wehner, R. (1997). The ant's celestial compass system: Spectral and polarization channels. In *Orientation and communication in arthropods* (pp. 145–185). Berlin, Heidelberg: Springer.

Wehner, R. (2003). Desert ant navigation: How miniature brains solve complex tasks. *Journal of Comparative Physiology A*, 189(8), 579–588.

Wehner, R., & Muller, M. (2006). The significance of direct sunlight and polarized skylight in the ant's celestial system of navigation. *Proceedings of the National Academy of Sciences of the United States of America*, 103(33), 12575–12579.

Wehner, R. (2009). The architecture of the desert ant's navigational toolkit (Hymenoptera: Formicidae). *Myrmecological News*, 12(September), 85–96.

Wehner, R., Hoinville, T., Cruse, H., & Cheng, K. (2016). Steering intermediate courses: Desert ants combine information from various navigational routines. *Journal of Comparative Physiology A*, 202(7), 459–472.

Wicklein, M., & Strausfeld, N. J. (2000). Organization and significance of neurons that detect change of visual depth in the hawk moth Manduca sexta. *Journal of Comparative Neurology*, 424(2), 356–376.

Witthöft, W. (1967). Absolute anzahl und verteilung der zellen im him der honigbiene. *Zeitschrift für Morphologie der Tiere*, 61(1), 160–184.

Wittlinger, M., Wehner, R., & Wolf, H. (2006). The ant odometer: Stepping on stilts and stumps. *Science*, 312(5782), 1965–1967.

Wolf, H., Wittlinger, M., & Pfeffer, S. E. (2018). Two distance memories in desert ants—Modes of interaction. *PLoS One*, 13(10), e0204664.

Wong, A. M., Wang, J. W., & Axel, R. (2002). Spatial representation of the glomerular map in the Drosophila protocerebrum. *Cell*, 109(2), 229–241.

Wu, M., Nern, A., Williamson, W. R., Morimoto, M. M., Reiser, M. B., Card, G. M., & Rubin, G. M. (2016). Visual projection neurons in the Drosophila lobula link feature detection to distinct behavioral programs. *Elife*, 5, e21022.

Yilmaz, A., Lindenberg, A., Albert, S., Grübel, K., Spaethe, J., Rössler, W., & Groh, C. (2016). Age-related and light-induced plasticity in opsin gene expression and in primary and secondary visual centers of the nectar-feeding ant Camponotus rufipes. *Developmental Neurobiology*, 76(9), 1041–1057.

Zeil, J., & Fleischmann, P. N. (2019). The learning walks of ants (Hymenoptera: Formicidae). *Myrmecological News*, 29, 93–110.

Zeller, M., Held, M., Bender, J., Berz, A., Heinloth, T., Hellfritz, T., & Pfeiffer, K. (2015). Transmedulla neurons in the sky compass network of the honeybee (*Apis mellifera*) are a possible site of circadian input. *PLoS One*, 10(12), e0143244.

Zieger, E., Bräunig, P., & Harzsch, S. (2013). A developmental study of serotonin-immunoreactive neurons in the embryonic brain of the Marbled Crayfish and the Migratory Locust: Evidence for a homologous protocerebral group of neurons. *Arthropod Structure & Development*, 42(6), 507–520.

Zube, C., Kleineidam, C. J., Kirschner, S., Neef, J., & Rössler, W. (2008). Organization of the olfactory pathway and odor processing in the antennal lobe of the ant Camponotus floridanus. *Journal of Comparative Neurology*, 506(3), 425–441.